

# A scanner-based rhizobox system enabling the quantification of root system development and response of *Brassica rapa* seedlings to external P availability

Michael O. Adu<sup>1,2,3</sup>, David O. Yawson<sup>1,4</sup>, Malcolm J. Bennett<sup>2</sup>, Martin R. Broadley<sup>2</sup>, Lionel X. Dupuy<sup>1</sup> and Philip J. White<sup>1,5</sup>

<sup>1</sup>Department of Ecological Sciences, The James Hutton Institute, Invergowrie, Dundee, DD2 5DA, UK

<sup>2</sup>Plant and Crop Sciences Division, School of Biosciences, University of Nottingham, Sutton Bonington Campus, Leicestershire, LE12 5RD, UK

<sup>3</sup>Department of Crop Science, School of Agriculture, College of Agriculture and Natural Sciences, University of Cape Coast, Cape Coast, Ghana

<sup>4</sup>Department of Soil Science, School of Agriculture, College of Agriculture and Natural Sciences, University of Cape Coast, Cape Coast, Ghana

<sup>5</sup>Distinguished Scientist Fellowship Program, King Saud University, Riyadh 11451, Kingdom of Saudi Arabia

Corresponding author: M. O. Adu, E-mail: michael.adu@ucc.edu.gh, Phone: +233-3321-91975, Fax: +233-3321-32709

Received on July 19, 2016; Accepted on Jan 6, 2017

**Abstract:** Rhizoboxes are soil-root compartments that may well provide the closest naturalistic conditions for studying root systems architectures (RSAs) in controlled environments. Rhizobox-based studies can however lead to mis-estimation of root traits due to poor recovery of roots and loss of fine root features during washing of roots. We used a novel scanner-based rhizobox system to evaluate: (i) RSA traits of *Brassica rapa* genotypes; (ii) the relationship between root traits recorded from rhizoboxes and those of harvested roots and (iii) genotypic variation of seedlings in response to external P ( $[P]_{\text{ext}}$ ) availability. *Brassica rapa* genotypes were grown in soil-filled rhizoboxes abutting flatbed scanners and were watered once with either deionised water or a solution of 600  $\mu\text{M}$   $\text{KH}_2\text{PO}_4$  to approximately 80% field capacity on a weight basis. Shoot and root P concentrations ( $[P]_{\text{shoot}}$  and  $[P]_{\text{root}}$ ) of the *B. rapa* lines grown on different  $[P]_{\text{ext}}$  were quantified. Visible root length at the surface of rhizoboxes constituted 85% of the total root length recovered from harvested root samples. High P supply induced a strong increase in  $[P]_{\text{shoot}}$  in all genotypes ( $P < 0.001$ ) whereas low P supply generally led to greater partitioning to roots. Seed P concentration and tissue P concentration were correlated only at low  $[P]_{\text{ext}}$ . Total root length was strongly correlated with tissue P content under both low  $[P]_{\text{ext}}$  ( $r = 0.81$ ,  $P < 0.05$ ) and

high  $[P]_{\text{ext}}$  ( $r = 0.82$ ,  $P < 0.05$ ) conditions. The novel scanner-based rhizobox system used addresses the substantial limitations associated with current use of rhizoboxes to study root growth dynamics.

**Keywords:** *Brassica rapa* L., nutrient acquisition, phosphorus, rhizobox, root system architecture, scanner-based phenotyping

**Abbreviations:** AIC, Akaike information criterion; BIC, Bayesian information criterion; CI, Confidence interval, CV; Coefficient of variation; DAS, Days after sowing on rhizobox; DW, Dry weight; FW, Fresh weight; LAUZ, Length of the apical unbranched zone; logLik, Log-likelihood; LRGR, Lateral root growth rate; LRL, Mean lateral root length; LRS, Lateral roots; NLR, Number of lateral Roots; PAR, Photosynthetic active radiation; PRL, Primary root length;  $[P]_{\text{ext}}$ , Soil or external phosphorus concentration;  $[P]_{\text{root}}$ , Root P concentration;  $[P]_{\text{shoot}}$ , Shoot P concentration; Q-Q, Quantile-quantile; R:S, Root-to-shoot ratio; RDW, Root dry weight; RFW, Root fresh weight; RILs, Recombinant inbred lines; RSA, Root system architecture; RTD, Root tissue density; SDW, Shoot dry weight; SFW, Shoot fresh weight; SRL, Specific root length; TLRL, Total lateral root length; TRL, Total root length; TVRL, Total visible root length

Adu M, Yawson D, Bennett M, Broadley M, Dupuy L, White P 2017 A scanner-based rhizobox system enabling the quantification of root system development and response of *Brassica rapa* seedlings to external P availability. Plant Root 11:16-32. doi:10.3117/plantroot.11.16

Copyrights 2017, Plant Root (JSRR), www.plantroot.org

## Introduction

The ability of plants to explore their soil environment for water and nutrients depends on the size and architecture of their root system (White et al. 2013b). Plants can adapt the growth and geometry of their root system (root system architecture, RSA) in response to the availability of water and nutrients in the soil environment (Hodge et al. 1999, White et al. 2013a, b). Hence, studying the responses of RSA to the availability of water and nutrients in the soil environment is crucial for developing crops that are resilient to abiotic stresses, effective in exploring the soil environment, and able to acquire and use resources efficiently to give good yields (Hodge et al. 1999, Lynch 2007, Ghanem et al. 2011, White et al. 2013a, b).

A common method for studying root systems of plants growing in soil is root excavation and washing of plants grown in the field (van Noordwijk et al. 2000, Gregory 2006). However, this approach is time-consuming and destructive because root washing causes breakage and loss of fine roots, resulting in underestimation of fine root features (Kosola et al. 2007, Mairhofer et al. 2013). High-throughput screening of root systems of juvenile plants in controlled environments is now possible as a result of recent advances in imaging techniques (Gregory et al. 2009, Dupuy et al. 2010a, b, Iyer-Pascuzzi et al. 2010, Dai et al. 2012, Galkovskiy et al. 2012, Nagel et al. 2012, Faget et al. 2013, Downie et al. 2015). New advances such as X-ray computed tomography (X-ray CT), X-ray microcomputed tomography, neutron tomography, magnetic resonance imaging (MRI), electromagnetic acoustic imaging, hyperspectral and 3-D meta material imaging are now providing higher resolution and improved clarity, enabling new modalities and facilitating enhanced portability (Asseng et al. 2000, Perret et al. 2007, Moradi et al. 2009, Tracy et al. 2010).

Root system phenotyping through imaging requires the use of uniform growth conditions. It also requires standard rooting medium that is affordable and provides repeatable root growth conditions (Crush et al. 2005, Adu et al. 2016). Quantitative imaging of roots requires imaging with good contrast between roots and their background to facilitate image analyses (Mairhofer et al. 2013, Adu et al. 2016). For these reasons, various rooting media have been used. Rooting media such as agar or gels (Jain et al. 2009, Yazdanbakhsh and Fisahn 2012, Gruber et al. 2013, Shi et al. 2013) and paper pouches (Liao et al. 2001, Hammond et al. 2009, Hund et al. 2009, Adu et al. 2014, 2015, 2016,

LeMarié et al. 2014, Kalogiros et al. 2016, Thomas et al. 2016) have been used successfully to screen plants for variation in RSA. However, such rooting media do not fully capture the soil properties, processes and conditions that prevail in the field, including microbial interactions and nutrient and water dynamics (Hutchings and John 2004, Nagel et al. 2009, Downie et al. 2015, Adu et al. 2016). Moreover, the mineral concentrations in commonly used artificial rooting media often differ from those found in soils (Jain et al. 2009, Gruber et al. 2013).

Soil-filled chambers (rhizoboxes) provide an alternative method for screening plant root systems in controlled environments under conditions closest to those prevailing in soils in the field. Rhizobox systems allow repeated, non-destructive and near-naturalistic measurements of root development and rhizosphere processes and could be said to be relatively more suited to field-grown roots than other artificial systems. Compared to soil in the field, roots can be recovered easily from soil-filled containers and such systems can be scaled up to accommodate a large number of plants. Rhizobox systems have thus become popular choice for root system studies. For example, soil-filled containers with transparent walls have been used to allow non-invasive, repeated measurements of the same roots on the surface of the containers at frequent time intervals for exploring the dynamics of water uptake (Garrigues et al. 2006, Neumann et al. 2009, Adu et al. 2016). Rhizoboxes have again been used to study the juvenile root system of field mustard (*Brassica rapa*), oilseed rape (*Brassica napus* L.) and Indian mustard (*Brassica juncea* L.) (Adu et al. 2016, Soledad et al. 2016, Yuan et al. 2016). Rhizoboxes have also been used to study the effect of root exudation from Indian mustard on soil solution properties such as pH, dissolved organic carbon (DOC) and metal solubility in the rhizosphere (Kim et al. 2010). Rhizoboxes have also been employed to study root proliferation in response to nutrient-rich patches in soils (Hodge et al. 1999) and the effects of soil compaction on RSA (Nagel et al. 2012).

However, despite their extensive use, most rhizoboxes still suffer from disturbance of soil structure, altered root-zone temperatures, limited rooting volume and two-dimensionality of the observation windows (Neumann et al. 2009). Most rhizoboxes allow only a fraction of the root system to be observed and it is not certain that data on RSA obtained from rhizoboxes are representative of the actual RSA of the plants (Nagel et al. 2012). Also, there is the tendency for roots to grow away from the surface of the containers, which causes difficulty with imaging. To address this challenge, the study described here adapted a scanner-based imaging

system (Adu et al. 2014, 2015) to study the root growth dynamics of *Brassica rapa* L. seedlings grown in rhizoboxes.

The objectives of this study were (i) to quantify the genotypic, environmental and temporal variation in root traits of plants grown in a soil-filled rhizobox, (ii) to assess whether the root system visible on the transparent surface of a rhizobox is representative of the actual root system of a plant and (iii) to assess the genotypic variation in RSA of seedlings in response to external P availability.

## Materials and Methods

### Phenotyping Platform

The phenotyping platform, comprising 24 soil-filled rhizoboxes attached to scanners, was constructed in a controlled environment room on a heavy-duty wire mesh (3.85 m × 1 m) raised 30 cm above the floor (Fig. 1A). Root growth was routinely monitored and captured with ArchiScan which has been installed on a computer directory on which there is sufficient space to save images (Adu et al. 2014, 2015, <http://www.archiroot.org.uk>). ArchiScan is fully parameterizable software which allows the management of several scanners for scheduled remote root growth acquisitions. The software has no limit to the number of scanners it can support. It

is generic and can be used with any scanner provided a TWAIN driver is available. The number of scanners per computer depends on the number of plants to be screened, duration of experiment, frequency of scanning and the computers' storage capacity. In our experiments, we used 3 computers to control 24 scanners. To set up an automated time-lapse image acquisition, input parameters of the new project for example included initial scanning time, project duration/frequency of image acquisition, and desired image parameters (including colour, resolution, scaling, frame size, brightness, contrast, file format etc.)

Lighting in the growth room was provided by 100 W cool-white fluorescent tubes (Philips, Eindhoven, Netherlands), with photosynthetic active radiation (PAR) of  $100 \pm 15 \mu\text{mol m}^{-2} \text{s}^{-1}$  (mean  $\pm$  standard deviation) at plant height (about 90 cm). In a pre-trial experiment, lighting in the growth room was provided by a Philips SON-T Agro 400-W high pressure sodium lamp with an illumination of  $550 \mu\text{mol m}^{-2} \text{s}^{-1}$  PAR (s.d.  $\pm 12 \mu\text{mol m}^{-2} \text{s}^{-1}$ ) at plant height. Problems with the initial lighting were basis for our choice of the later lighting system. We opted for the 100 W cool-white fluorescent tubes because the distance between plants the light was short and as a result, the original lamps (the Philips SON-T Agro 400-W high pressure sodium lamp) produced excessive heat and condensation on the scanner

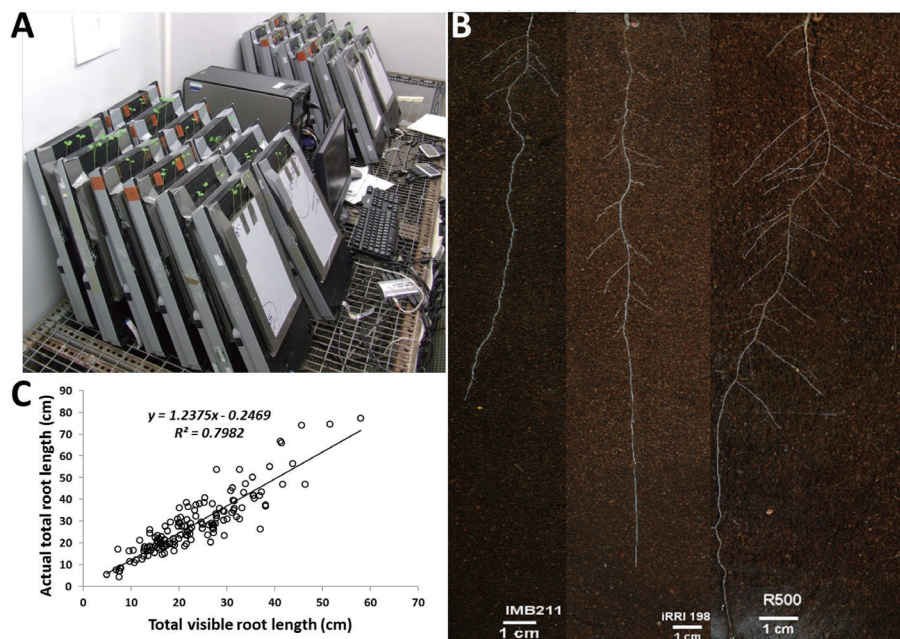


**Fig. 1.** (A) System for phenotyping roots in soil-filled rhizoboxes showing 24 scanners arranged in rows of 6. The angle of inclination of the scanners and hence rhizoboxes was approximately 80°; (B) Example of root systems of *Brassica rapa* L. seedlings 15 d after sowing. R500 and IMB211 are parents and IRR1198 is a recombinant inbred line from the BraIRRI mapping population; (C) Relationship between total visible root length on the transparent surface of soil-filled rhizoboxes and total harvested root length of *Brassica rapa* seedlings grown for 15 d after sowing.

window. To determine the suitability of the 100 W cool-white fluorescent tubes, we conducted a preliminary trial and compared stem elongation, development and shape of leaves and root growth of glasshouse-grown seedlings with that of seedlings grown in our growth room. The results (data not shown) did not suggest any possible effect of the low light conditions provided by the 100 W cool-white fluorescent tubes on the traits examined. The growth room air temperature was maintained at  $15 \pm 1^\circ\text{C}$  and relative humidity at  $60 \pm 5\%$  during the 16/8 h light/dark cycle. The rhizoboxes, adapted from Bengough et al. (2004), were constructed from two polyvinylchloride plates measuring  $30 \times 21.5 \times 0.3$  cm, one of which was opaque and the other transparent. The two polyvinylchloride plates were separated by spacers made of strips of Perspex,  $0.3 \times 0.3 \times 30$  cm and  $0.3 \times 0.3 \times 21.5$  cm, respectively, placed along the long-edges and short-edges of each plate, giving a separation of the two plates of 0.6 cm. Three gaps, each approximately 3 cm long, were left along the top edge to allow gas exchange with the surrounding atmosphere and unimpeded shoot growth. The spacers at the bottom of each soil-filled box had holes to allow free gravity drainage of water and improved aeration. Roots grew near the surface of the rhizobox windows for continued optical observation of the root-soil interface zone and non-destructive measurements of root growth dynamics along the observation window.

#### Soil Characteristics

Each rhizobox was filled with topsoil collected from the 0 to 10 cm horizon of a cultivated field at Tayport ( $56.45^\circ$  N,  $2.88^\circ$  W), Scotland. The soil was typical of arable soil of the region and plants grown on this soil have previously been shown to respond to P fertilisation (George et al. 2011). The soil was characterised as a sandy loam with a pH of 6.3 and total digestible P (Total P or acid digestible P) of  $1475 \text{ mg P kg}^{-1}$  of which 40.8% was in organic moieties. The soil had Olsen P, water extractable inorganic P, and organic P concentrations of 84.5 (probably due to applications of pig manure), 6.3 and  $0.5 \text{ mg P kg}^{-1}$ , respectively (George et al. 2011, Brown et al. 2012). Soil was air-dried, mixed and passed through a 2 mm sieve to remove coarse inorganic and organic matter. Sieved soil was loosely packed into each rhizobox at a dry bulk density of approximately  $1.0 \text{ g cm}^{-3}$  and occupied a volume of approximately  $300 \text{ cm}^3$ . The soil in each rhizobox was watered once with either deionised water (un-amended soil, low  $[\text{P}]_{\text{ext}}$ ) or a solution of  $600 \mu\text{M KH}_2\text{PO}_4$  (amended soil, high  $[\text{P}]_{\text{ext}}$ ) to approximately 80% field capacity on gravimetric

water content basis immediately prior to planting pre-germinated seeds.

#### Characterisation of RSA

The parents and ten recombinant inbred lines (RILs) of the BraIRRI mapping population of *Brassica rapa* L. (Iniguez-Luy et al. 2009) were used in this study. Seeds were pre-germinated on  $12 \text{ cm} \times 12 \text{ cm}$  germination papers (Anchor Paper Co., Saint Paul, MN, USA). The germination paper was sprayed with de-ionised water and placed in a near vertical position in a Sanyo MIR153<sup>®</sup> incubator at  $15^\circ\text{C}$ . Three days after sowing, seedlings of similar size with radicles 2–3 cm in length were transferred to rhizoboxes for experiments. In a completely randomized design, three seedlings of the same genotype were placed on each soil-filled box attached to a scanner and there were two scanners per genotype. Two separate experiments were performed. In both experiments, 24 rhizoboxes were sown each containing three seedlings of a particular genotype.

#### Experiment 1: Genotypic, environmental and temporal variation in RSA

Genotypic, environmental and temporal variation in the root system of randomly selected *Brassica rapa* L. genotypes was determined. These genotypes comprised the parents (cv. IMB211, cv. R500) and 10 RIL (IRRI002, IRRI016, IRRI030, IRRI104, IRRI124, IRRI198, IRRI201, IRRI229, IRRI360, IRRI380) of the *B. rapa* recombinant inbred (BraIRRI) mapping population (Iniguez-Luy et al. 2009). The BraIRRI population is a fixed mapping population consisting of 160 recombinant inbred lines (RILs) derived from the cross between IMB211 and R500 (Iniguez-Luy et al. 2009). Genotype IMB211 is a highly inbred rapid cycling Chinese cabbage *B. rapa* subsp. *pekinensis* and R500 is a highly inbred annual yellow sarson *B. rapa* subsp. *trilocularis* (Iniguez-Luy et al. 2009, Xu et al. 2010).

Six seedlings of each genotype were grown on un-amended soil in each of two independent runs. Images of root system architecture (RSA) of seedlings were collected daily for 15 days after transfer to the rhizobox (DAS). Plants were harvested 15 DAS. Each plant was separated into shoot and root samples. The fresh weight (FW) of shoot material was determined immediately and the FW of root material was determined after RSA traits (e.g.: total root length, root volume, surface area) were measured using WinRhizo (Version 2012b; Regent Instruments, Quebec City, Canada). Shoot

and root material were dried at 70°C for 3 days, and their dry weight (DW) determined.

#### *Experiment 2: Effect of soil P concentration ( $[P]_{\text{ext}}$ ) on RSA*

The effect of soil P concentration ( $[P]_{\text{ext}}$ ) on RSA was determined for six *Brassica rapa* L. genotypes found to have contrasting RSA in Experiment 1. These genotypes were the parents (cv. R500, IMB211) and four RIL (IRRI016, IRRI124, IRRI201, IRRI229). Plants were either grown on unamended soil (low  $[P]_{\text{ext}}$ ) or on soil watered with a solution of 600  $\mu\text{M}$   $\text{KH}_2\text{PO}_4$  (high  $[P]_{\text{ext}}$ ). Six seedlings of each genotype were grown in two independent runs. Images of RSA were collected daily for 21 DAS and plants were harvested 21 DAS. Each plant was separated into shoot and root samples. The FWs of these samples were determined, before they were dried at 70°C for three days and their DWs determined. Dried samples were acid-digested as described by Brown et al. (2012) and shoot P concentration ( $[P]_{\text{shoot}}$ ) and root P concentration ( $[P]_{\text{root}}$ ) were determined using the Malachite green assay of Irving and McLaughlin (1990). Seed P concentrations of the six genotypes used for Experiment 2 was also determined. Here, the Malachite green assay of Irving and McLaughlin (1990) was employed to determine the seed P of representative seed samples from those used as planting materials in Experiment 2. Dry weight per 10 seeds for each of the six genotypes was also determined.

#### *Time-lapse imaging of roots*

Root growth was automatically imaged with A4 CanoScan 5600F flatbed scanners (Canon UK Ltd, Reigate, UK). Rhizoboxes were fixed to scanners using duct tape with the transparent wall aligned with the glass window of the scanner (Fig. 1A). Images were taken daily in the middle of the light period. The frequency of image acquisition, scanning resolution, and file format was controlled by three computers using the custom software ArchiScan.

#### *Measurement of RSA traits*

Root traits (length, area, volume and diameters) of plants were measured at harvest using WinRhizo (Version 2012b). Root systems of individual plants were placed in 150 mm polystyrene Petri dishes containing water and scanned using an Epson Expression 10000XL scanner (Epson UK, London). Images were converted to a binary image using a

grey value threshold of 30 and objects with an area  $<1 \text{ cm}^2$  and a length-to-width ratio  $<4$  were removed (Nagel et al. 2012). Information on RSA was extracted from images captured with flatbed scanners during the experiments using SmartRoot software (Lobet et al. 2011). SmartRoot was used to extract traits such as primary root length (PRL), branching density (B. Dens.), number of lateral roots (NLR), mean lateral root length (LRL), root insertion angle (angle), interbranch distance (Int. Dist.), length of the apical unbranched zone (LAUZ) and total root length (TRL) and total lateral root length (TLRL).

#### *Statistical analysis*

Descriptive statistics for all traits were calculated. An estimate of the standard deviation ( $\sigma$ ) and the mean ( $\pm$  standard error) were obtained and the coefficient of variation (CV) was determined as the standard deviation divided by the mean and expressed as a percentage. Root trait data from the parents of the population (cv. R500 and IMB211) in Experiment 1 were used to calculate the number of replicates (N) that would be required to detect a significant difference between the means of two populations with identical standard deviations in a trait using a two-sided, 95% confidence interval (CI) *t*-test, if the trait means differed by 50% using Supplemental equation S1. Pearson's correlation coefficients between all trait combinations were determined.

Genotypic variability was analysed using three-way ANOVA. The sources of variation in static root traits (i.e. root traits measured on the last day of the experiment) were determined using a mixed effects model as described by Adu et al. (2014). The run, scanner and genotype were considered as random factors using Supplemental equation S2. Phenotypic variance was then calculated with the estimated genetic variance ( $\sigma_g^2$ ), genotype  $\times$  run variance ( $\sigma_{ag}^2$ ) and the error variance ( $\sigma_\epsilon^2$ ) using Supplemental equation S3. Broad-sense heritability ( $H^2$ ) was estimated as  $\sigma_g^2/\sigma_p^2$ , where  $\sigma_g^2$  is the estimated variance associated with the genotypic effect and  $\sigma_p^2$  is the total variance for the trait.

The sources of variation in dynamic root traits (i.e. root traits determined throughout the growth period) were determined using mixed effects models incorporating both fixed and random effects as described by Adu et al. (2014). Genotype and run were considered as random factors and to account for non-linearity in growth curves, a logistic growth function was used to model the increase in total root length (TRL) and primary root length (PRL) with time using Supplemental

equation S4. The three parameters of the logistic function were the asymptote ( $\Phi_1$ ), inflection point ( $\Phi_2$ ), and scale parameter ( $\Phi_3$ ). To account for heteroscedasticity in the models, a power variance function of the form shown in the Supplemental equation S5 was used. The sources of variation in the growth rate of lateral roots were determined using Supplemental equation S6. Data for growth rates of lateral roots were normalized by square root transformation. Adequacy and quality of the models for TRL, PRL and lateral root growth rate (LRGR) was assessed by log-likelihood (logLik), Akaike information criterion (AIC), Bayesian information criterion (BIC) and quantile-quantile (Q-Q) plots (Pinheiro and Bates, 2000, Adu et al. 2014).

Data for shoot and root biomass, and the length of the total root system, were log-transformed to linearize these data before statistical analyses in Experiment 2, but frequency distributions indicated that neither of the remaining traits in Experiment 2 nor any trait measured in Experiment 1 required transformation (data not shown). A mixed effect model was used to analyse static root data using Supplemental equation S7 and the mean trait value for genotypes was determined using the  $[(P]_{\text{ext}} \times \text{genotype}]$  term as a fixed factor retaining  $[\text{run} \times$

$[(P]_{\text{ext}} \times \text{genotype}]$  as a random factor (Shi et al. 2013). Statistical analyses were performed using GenStat (GenStat Release 14.1, VSN International, Oxford, UK) and the nlme library in the R software (Pinheiro and Bates 2000, Pinheiro et al. 2008). Regressions were executed between seed P, seed mass and tissue P.

## Results

### Experiment 1

#### *A rhizobox platform for high-resolution quantification of RSA development*

In this study, only the roots reaching the surface of the observation windows of the rhizobox can be observed and measured through image analysis (Fig. 1B). Total root length (TRL) was mostly larger than total visible root length (TVRL). In a few of the dataset (8.3% of measurements taken), TVRL was larger than TRL for the corresponding plant. This suggests that in such occurrences, some roots may have been left in the soil or lost during washing. The proportion of roots reaching the surface of the observation window (total visible root length)

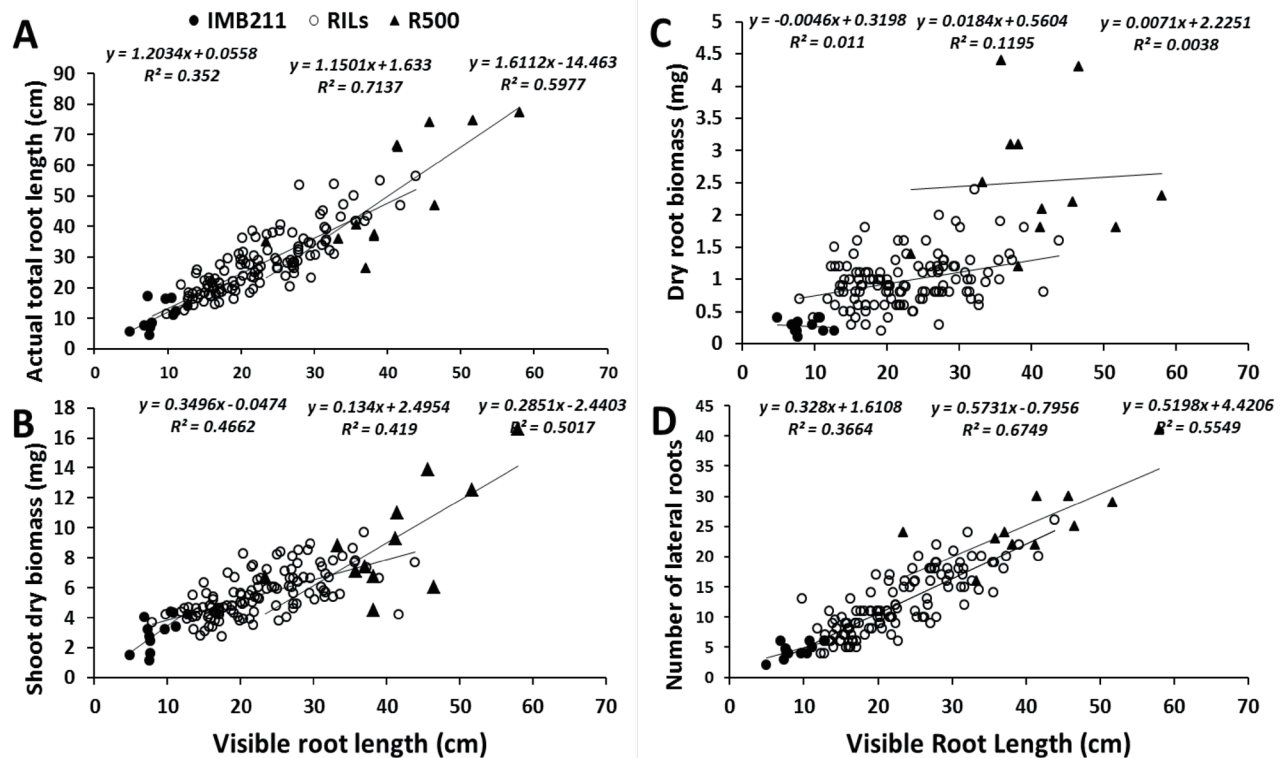


Fig. 2. Correlation between root lengths visible at the transparent surface of soil-filled rhizoboxes with (A) harvested total root-system lengths; (B) shoot biomass; (C) root biomass and (D) number of lateral roots. Open circles, filled circles and filled triangles are data points for IMB211, RILs and R500, respectively; Equations and  $R^2$  values on each plot are from left to right on each chat, the trend lines of IMB211, RILs and R500, respectively.

ranged from 78 to 93% and were 93.0, 83.9, 82.6, 81.4, 79.0, 84.3, 90.3, 92.2, 78.0, 91.0, 78.4 and 85.5%, respectively for IMB211, IRR1002, IRR1016, IRR1030, IRR1104, IRR1124, IRR1198, IRR1201, IRR1229, IRR1360, IRR380 and R500. On average, 85% of the TRL was visible on the surface of the observation window (i.e. TVRL). There was a linear relationship ( $r = 0.90$ ) between TVRL and TRL with a slope of 0.65 for all the genotypes combined (Fig. 1C). The correlation coefficients ( $r$ ) for the relationship between TVRL and TRL for the parental genotypes were 0.60 and 0.77, respectively. The correlation coefficient ( $r$ ) for the relationship between the TVRL and the TRL for the RILs combined was 0.82, suggesting that about 33% of variation of TVRL ( $1 - 0.82^2$ ) is due to other variables than TRL. However, the correlation coefficient ( $r$ ) for the relationship between the TVRL and TRL differed between genotypes, which may be a consequence of differences in the size of the root system between genotypes or differences in root diameter or other aspects which would likely induce different proportions of TVRL and TRL. Slopes of linear regressions between TVRL and TRL also varied between genotypes, with values of 1.20, 1.61 and 1.15 recorded for IMB211, R500 and all RILs combined, respectively (Fig. 2). Total visible root length also correlated well with traits such as shoot biomass, root biomass and number of lateral roots and could, therefore, be explored as proxies for those traits. However, these relationships were also influenced by the genotype (Fig. 2). Correlation coefficients ( $r$ ) for the relationships between TVRL and shoot biomass and number of lateral roots were 0.68 and 0.61, respectively, for parental genotype IMB211; 0.71 and 0.74, respectively, for parental genotype, R500; and 0.65 and 0.82, respectively, for the 10 RILs combined. The correlation coefficients ( $r$ ) for the relationship between TVRL and root biomass was the lowest of all traits studied (Fig. 2).

#### *Requisite replication*

Between 4 (calculated for number of lateral roots) and 48 (calculated for root-to-shoot ratio) replicates, depending upon the trait, would be required to detect a significant difference in means of two genotypes using a 2-sided, 95% CI,  $t$ -test if trait means differed by 50% (Supplemental Table S1). Differences between means for certain traits including branching density, lateral root insertion angle, mean inter-branch distance and specific root length were very small and for such traits, estimated sample sizes required to detect a significant difference in means of two genotypes using a 2-sided, 95% CI,  $t$ -test if trait means differed by

50% were large (Supplemental Table S1). This could be due to an inability to detect some root axes on the surface of the rhizobox or essentially small differences for these variables.

#### *Sources of variation in static root traits*

Most of the variation in all root traits could be attributed to the genotype and experimental conditions (i.e. run and block). Genotypic variation comprised 0–39% of the overall trait variation. The parental genotypes exhibited extreme values for many biomass and root architectural traits with the R500 and IMB211 genotypes having the greatest and smallest values, respectively, for the majority of root and shoot traits. However, there was evidence of transgressive segregation in some traits, where some RILs exhibited phenotypes that were extreme relative to the parental genotypes. Although this will be more relevant with whole population and not 12 genotypes, transgression was observed in traits such as branching density, mean lateral root (LR) length, LR insertion angle and LR inter-branch distance (Supplemental Table S2). The effects of genotype, and the effects of interactions between genotype  $\times$  run, genotype  $\times$  block and genotype  $\times$  run  $\times$  block accounted for most of the variation in the experiment (Table 1). Broad-sense heritability was greatest for root biomass traits ( $>0.84$ ), PRL (0.88) and total lateral root length (TLRL, 0.76), intermediate (0.40–0.68) for shoot biomass, mean LRL (0.65) and length of the apical unbranched zone (LAUZ, 0.64), and lowest ( $<0.4$ ) for branching density and root volume (Table 1).

#### *Relationships between measured traits*

There were strong positive correlations among biomass traits for the 144 plants studied (Fig. 3). There were also strong correlations between biomass and root architectural traits (Fig. 3). Total root length was positively correlated with shoot fresh weight (SFW;  $r = 0.85$ ;  $P < 0.05$ ), shoot dry weight (SDW;  $r = 0.81$ ;  $P < 0.05$ ), root fresh weight (RFW;  $r = 0.83$ ;  $P < 0.05$ ). Within root traits, TRL strongly correlated with root surface area ( $r = 0.86$ ;  $P < 0.05$ ), PRL ( $r = 0.75$ ;  $P < 0.05$ ), number of lateral roots (LRs;  $r = 0.75$ ;  $P < 0.05$ ) and TLRL ( $r = 0.85$ ;  $P < 0.05$ ). Root FW showed strong positive correlation with PRL ( $r = 0.77$ ;  $P < 0.05$ ) and TLRL ( $r = 0.77$ ;  $P < 0.05$ ). Other significant positive correlations included that between TLRL and number of LRs ( $r = 0.75$ ;  $P < 0.05$ ), PRL and number of LRs ( $r = 0.76$ ;  $P < 0.05$ ), TLRL and PRL ( $r = 0.65$ ;  $P < 0.05$ ). Significant correlations were also recorded between root-to-shoot ratio (R:S) and specific root length (SRL;  $r = -0.67$ ;  $P < 0.05$ ) (Fig. 3).

**Table 1.** Sources of variation and broad sense heritability ( $H^2$ ) in shoot and root traits among 144 seedlings (12 replicate seedlings each of the parents and 10 recombinant inbred lines of the *Brassica rapa* BraIRRI mapping population) grown for 15 days after transfer to the rhizobox in two runs each of six blocks in soil-filled rhizoboxes

Measured Trait <sup>a</sup>	Standard deviations of effects					$H^2$	Source of variation (%)				
	$\sigma_g$	$\sigma_{ag}$	$\sigma_{bg}$	$\sigma_{abg}$	$\sigma_e$		Genotype	Genotype × Run	Genotype × Block	Genotype × Run × Block	Residual
SFW (mg)	30.74	28.54	0.00	11.09	24.04	0.68	32.56	30.23	0.00	11.74	25.47
SDW (mg)	1.24	1.29	0.00	0.14	1.30	0.64	31.20	32.57	0.00	3.56	32.67
RFW (mg)	4.55	1.13	0.00	2.67	3.25	0.89	39.18	9.75	0.00	23.04	28.03
RDW (mg)	0.48	0.13	0.00	0.36	0.33	0.84	36.86	10.06	0.00	27.55	25.53
TRL (cm)	6.25	9.70	0.00	4.45	6.87	0.42	22.91	35.57	0.00	16.32	25.20
Mean Diam. (mm)	0.00	0.00	0.00	0.03	0.02	0.00	0.00	0.00	4.66	55.09	40.25
Surf. Area (cm <sup>2</sup> )	0.00	0.97	0.20	0.31	0.82	0.00	0.00	42.03	8.84	13.41	35.72
Root Vol. (cm <sup>3</sup> )	2.11	7.72	0.00	7.56	5.50	0.09	9.22	33.74	0.00	33.03	24.01
PRL (cm)	3.25	1.17	0.00	1.61	2.33	0.88	38.91	13.98	0.00	19.23	27.88
B. Dens. (root cm <sup>-1</sup> PRL)	0.13	0.14	0.00	0.31	0.44	0.31	12.71	13.96	0.00	30.04	43.29
NLR	4.69	1.79	0.70	1.85	3.79	0.88	36.60	13.95	5.47	14.42	29.56
Mean LRL (cm)	0.13	0.12	0.01	0.05	0.23	0.65	23.61	21.53	1.66	9.99	43.20
Angle (°)	0.66	2.74	1.48	0.00	6.06	0.07	6.06	25.02	13.55	0.00	55.37
Int. Dist. (cm)	0.15	0.15	0.13	0.11	0.27	0.49	18.82	18.22	16.01	13.71	33.24
LAUZ (cm)	0.91	0.82	0.33	0.00	1.89	0.64	22.99	20.77	8.44	0.00	47.79
TLRL (cm)	6.00	4.14	0.00	2.81	6.45	0.76	30.91	21.32	0.00	14.51	33.26
SRL (cm mg <sup>-1</sup> SDW)	0.00	16.66	0.00	4.96	10.48	0.00	0.00	51.91	0.00	15.45	32.64
R:S	0.00	0.07	0.00	0.05	0.06	0.00	0.00	40.78	0.00	25.50	33.73

<sup>a</sup>Abbreviations: Shoot Fresh Weight (SFW), Shoot Dry Weight (SDW), Root Fresh Weight (RFW), Root Dry Weight (RDW), Total Root Length (TRL), Mean Root Diameter (Mean Diam.), Total Surface Area of Root (Surf. Area), Root Volume (Root Vol.), Primary Root Length (PRL), Branching Density (B. Dens.), Number of Lateral Roots (NLR), Mean Lateral Root Length (LRL), Root Insertion Angle (Angle), Lateral Root Interbranch Distance (Int. Dist.), Length of the Primary Root Apical Unbranched Zone (LAUZ), Total Lateral Root Length (TLRL), Specific Root Length (SRL), RDW/SDW (R:S).

$\sigma_g^2$  = estimated variance associated with the effect of genotype,  $\sigma_{ag}^2$  = estimated covariance associated with the effect of genotype × experimental run,  $\sigma_{bg}^2$  = estimated covariance associated with the effect of genotype × block,  $\sigma_{abg}^2$  = estimated covariance associated with the effect of genotype × experimental run × block,  $\sigma_e^2$  = estimated variance associated with the residual error,  $H^2$  = broad-sense heritability.

**Table 2.** Estimates of the asymptotes and inflection points ( $\Phi_{i1}$  and  $\Phi_{i2}$  in the Supplemental equation S4) for mixed effects models describing temporal variation in Total Root Length (TRL), the asymptote ( $\Phi_1$  in the Supplemental equation S4) for Primary Root Length (PRL), and the intercept ( $b_{i1} + \beta_1$ , Supplemental equation S6) for mixed effects models describing the growth rate of lateral roots (LGR), among the parents (IMB211, R500) and 10 recombinant inbred lines of the *Brassica rapa* BraIRRI mapping population grown for 15 days after transfer to soil-filled rhizoboxes

	IMB 211	R 500	IRRI 002	IRRI 016	IRRI 030	IRRI 104	IRRI 124	IRRI 198	IRRI 201	IRRI 229	IRRI 360	IRRI 380
TRL												
Asymptote ( $\Phi_{i1}$ )	9.02	61.59	35.75	29.45	23.00	37.20	35.43	31.84	41.24	29.69	42.01	24.52
Inflection ( $\Phi_{i2}$ )	8.99	11.33	10.50	9.10	9.55	11.63	11.13	11.19	12.18	9.22	11.24	8.69
PRL												
Asymptote ( $\Phi_1$ )	8.89	31.91	17.52	16.44	15.99	23.73	18.71	18.61	18.38	16.95	20.17	18.53
LGR												
Intercept ( $b_{i1} + \beta_1$ )	0.071	0.086	0.079	0.080	0.083	0.080	0.083	0.091	0.083	0.085	0.075	0.086
PRL/TRL Asymptotes ( $\Phi_1/\Phi_{i1} \times 100$ )	99	52	49	56	70	64	53	58	45	57	48	76

The percentages of the asymptotic TRL made up of asymptotic PRL ( $\Phi_1/\Phi_{i1}$ ) are also indicated.



### The dynamics of root growth

Total root length increased sigmoidally for all genotypes in both runs (Supplemental Fig. S1). There was considerable variability, both in the asymptote of TRL and in its gradient over time. The best-fit model was obtained with models consisting of two random-effects parameters, the asymptote,  $\Phi_{11}$  and inflection point,  $\Phi_{12}$  (Supplemental equation S4), describing the effect of genotype on the maximum TRL and time measured in DAS at which 50% of the maximum TRL occurs. The parental genotypes, IMB211 and R500, recorded the smallest and largest asymptotes, respectively for TRL (Supplemental Fig. S1). Maximum TRL ranged from 9.0 to 62.0 cm and these were the values recorded by the parental genotypes IMB211 and R500, respectively. The inflection point of TRL ranged from 8.0 to 12 DAS with the parental genotypes, IMB211 and R500 having values of approximately 9 and 11 DAS, respectively. The

scale parameter of the logistic growth function for TRL ( $\Phi_3$ ), which represents time in days from the inflection point to the time when 73% of the maximum root length is achieved, was approximately 4 days across the genotypes.

Primary root length was a major contributor to TRL (PRL was 45–99%; Table 2), which might be a consequence of LRs being less visible at the surface of the rhizobox, particularly for the genotypes with smaller root systems (e.g. IMB211). Primary root length also increased sigmoidally for all genotypes in both runs (Supplemental Fig. S1). The most informative model for PRL was obtained from a model with only one random effect (asymptote,  $\Phi_1$ ; Supplemental equation S4) and this differed between genotypes ( $P < 0.05$ ) (Table 2). Asymptotes for PRL ranged from 8.9 (IMB211) to 31.9 (R500) cm. Values for the inflection point and scale parameter of the logistic growth function for PRL were constant and were approximately 8 DAS and 5, respectively.

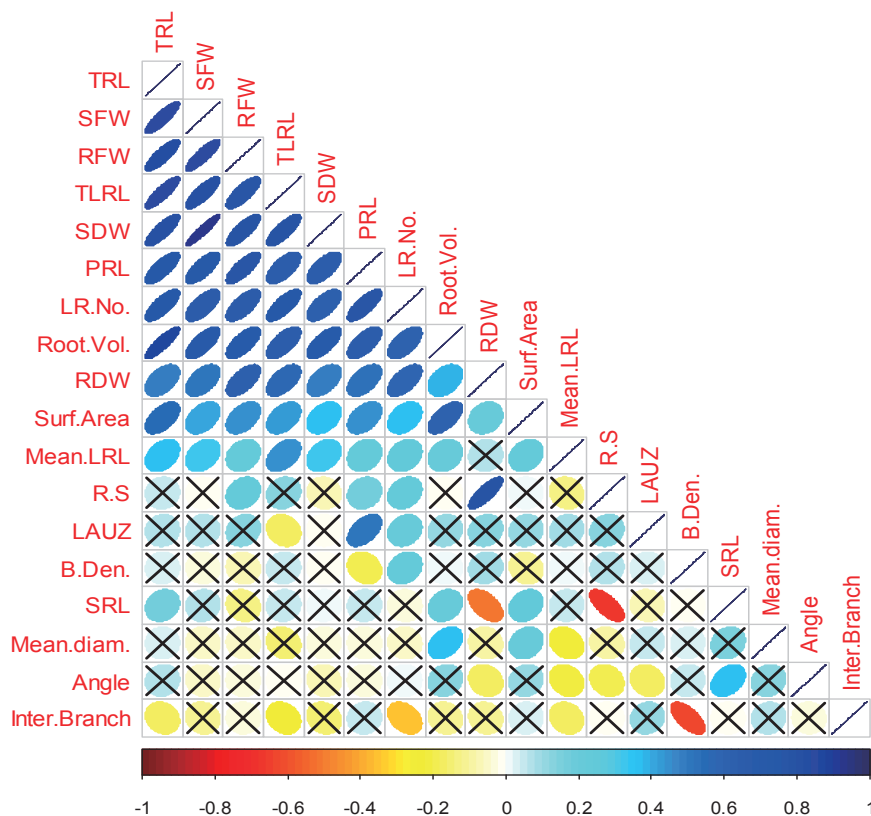


**Fig. 3.** Correlations between traits observed in plants grown in soil-filled rhizoboxes. Traits shown in the matrix are SFW: shoot fresh weight, SDW: shoot dry weight, RFW: root fresh weight, RDW: root dry weight, TRL: total root length, TLRL: total lateral root length, PRL: primary root length, Surf Area: root surface area, Root Vol.: root volume, Mean Diam.: mean root diameter, B. Dens.: branching density, LR No.: number of lateral roots, Mean LRL: mean lateral root length, Angle: mean insertion angle of lateral roots, Inter Branch: mean inter-branch distance between lateral roots, LAUZ: length of the apical un-branched zone of primary roots, R:S: root-to-shoot ratio and SRL: specific root length. Eccentricity and colour of the ellipses represents the correlation value. The scale is indicated in the bar below the matrix. Boxes with crosses indicate non-significant relationships ( $P < 0.05$ ).

Lateral root growth rate (LRGR) increased quadratically with time (DAS) for all genotypes (Supplemental Fig. S1). The most informative model included only one, random-effect parameter ( $b_{il}$ , Supplemental equation S6) describing the effect of genotype on the initial growth rate of LRs. The model also included a correlation structure and variance function. The initial LRGR ( $b_{il} + \beta_l$ ) differed between genotypes (Table 2). Values for  $b_{il} + \beta_l$  ranged from 0.071 (IMB211) to 0.091 (IRRI 198)  $\text{cm d}^{-1}$ . The other parental genotype, R500 had a value of 0.086  $\text{cm d}^{-1}$ . Model quality assessed with

logLik, AIC, BIC and Q-Q plots suggested that the models were satisfactory (data not shown).

### Experiment 2

#### Effect of genotype, external Pi concentration and their interactions

All genotypes responded to P supply. A linear relationship was observed between biomass of the six genotypes of *Brassica rapa* L. grown in soil with either 600  $\mu\text{M}$  of  $\text{KH}_2\text{PO}_4$  solution (high  $[\text{P}]_{\text{ext}}$ ) or 0

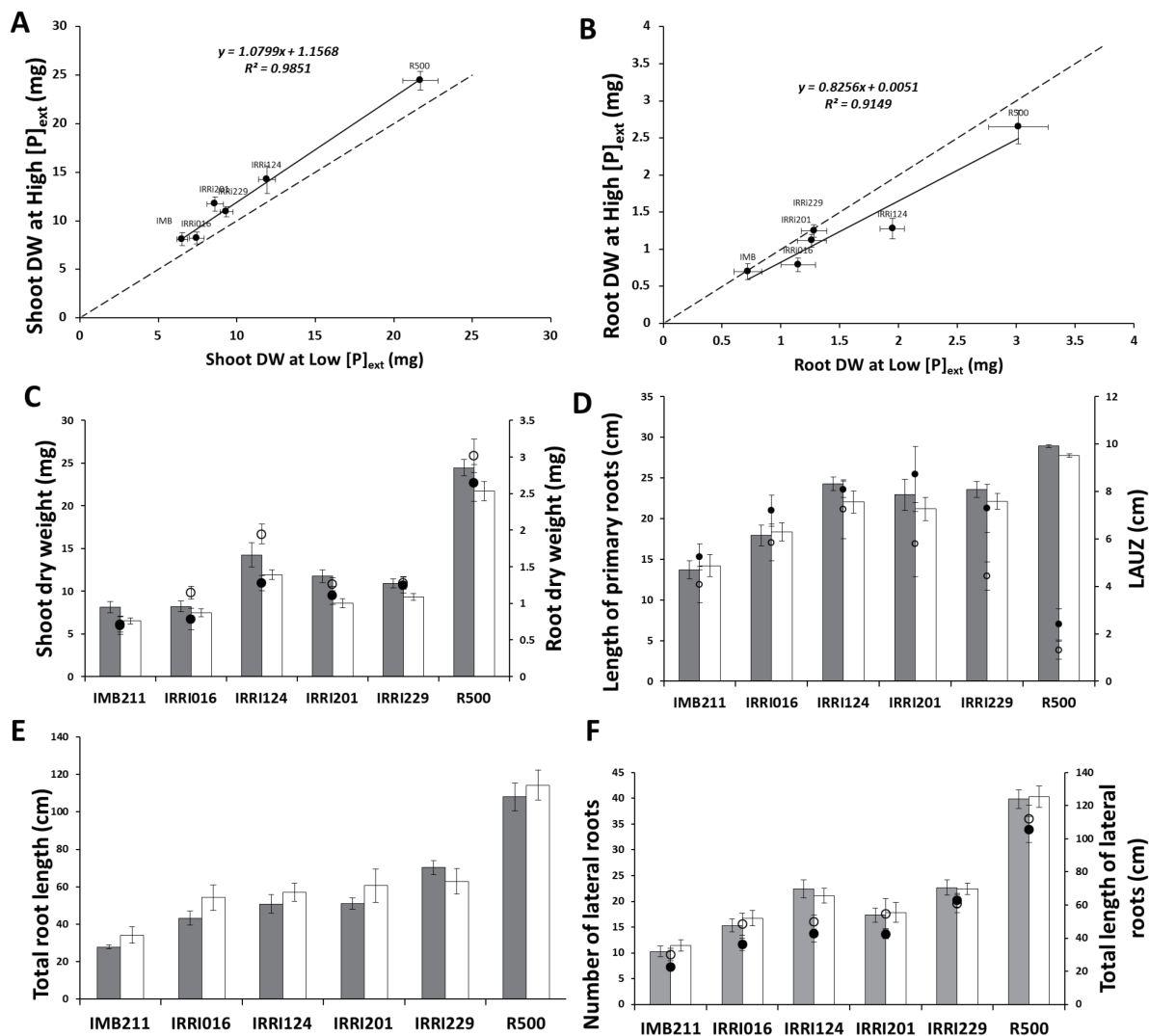


**Fig. 4.** Shoot and root traits for six *Brassica rapa* genotypes grown in soil-filled rhizoboxes at low  $[\text{P}]_{\text{ext}}$  (un-amended soil) and high  $[\text{P}]_{\text{ext}}$  (soil amended with solution containing 600  $\mu\text{M}$   $\text{KH}_2\text{PO}_4$ ) for 21 DAS. For all Figs where applicable, grey columns and filled circles are for plants grown on High  $[\text{P}]_{\text{ext}}$  soil and open columns and open circles are for plants grown under Low  $[\text{P}]_{\text{ext}}$  and symbols represent means  $\pm$  s.e.m. ( $n = 12$ ). (A) Relationship between shoot dry weight at low and high  $[\text{P}]_{\text{ext}}$ ; (B) Relationship between root dry weight at low and high  $[\text{P}]_{\text{ext}}$ . The dash line represents the 1:1 line; (C) Variation in shoot and root dry weight. Columns represent shoots and circles represent roots. (D) Variation in primary root length (PRL) and length of the apical unbranched zone of the primary root (LAUZ). Columns represent PRL and circles represent LAUZ. (E) Variation in total root length (TRL). (F) Variation in number of lateral roots (NLRs) and total lateral root length (TLRL). Columns represent NLRs and circles represent TLRL.

$\mu\text{M}$  of  $\text{KH}_2\text{PO}_4$  (low  $[\text{P}]_{\text{ext}}$ ) (Fig. 4A, 4B). Correlations between low  $[\text{P}]_{\text{ext}}$  and high  $[\text{P}]_{\text{ext}}$  treatments for biomass were significant ( $P < 0.001$ ; Fig. 4A, 4B). Genotypes grown on high  $[\text{P}]_{\text{ext}}$  soil yielded between 13 and 36% greater SDW but between 3 and 53% less RDW than lines grown on low  $[\text{P}]_{\text{ext}}$  soil (Fig. 4A, 4B, 4C). While the effect of  $[\text{P}]_{\text{ext}}$  did not alter PRL significantly, it affected LAUZ significantly ( $P < 0.001$ ). The LAUZ was 28.4, 22.9, 11.7, 50.6, 64.2 and 81.8% greater in seedlings of IMB211, IRR1016, IRR1124, IRR1201, IRR1229 and R500 grown on high  $[\text{P}]_{\text{ext}}$  soil compared to those grown on low  $[\text{P}]_{\text{ext}}$  soil, respectively (Fig. 4D). At high  $[\text{P}]_{\text{ext}}$ , the roots accounted for approximately 8 to 10% of total biomass in various lines compared to 10 to 14% at low  $[\text{P}]_{\text{ext}}$ . Total root length was significantly reduced in three of the six lines assayed at high  $[\text{P}]_{\text{ext}}$  compared with low  $[\text{P}]_{\text{ext}}$  (Fig. 4E). Seedlings grown

on high  $[\text{P}]_{\text{ext}}$  soil had less TLRL than those grown on low  $[\text{P}]_{\text{ext}}$  soil in majority of the genotypes studied (Fig. 4F). Whilst mean diameter and volume of roots were on average reduced when plants were grown on low  $[\text{P}]_{\text{ext}}$  soil, root tissue density (RTD, the ratio of root dry mass to root volume) and the ratio of root surface area to root volume were generally greater ( $P < 0.001$ ) when plants were grown on low  $[\text{P}]_{\text{ext}}$  soil (Supplemental Fig. S2).

Genotypic effects accounted for the largest proportion of total variance in SDW (78%), RDW (64%), number of LRs (76%), PRL (59%) and TRL (56%) (Supplemental Table S3). Genotype accounted for less variance in average diameter, angle, inter-branch distance, branching density, and R:S. Less variation was attributed to  $[\text{P}]_{\text{ext}}$  than genotype, including 5% for SDW, 19% for average diameter, 10% for LAUZ, 23% for branching density, 30% for R:S, 18% for root area to volume ratio and 19% for

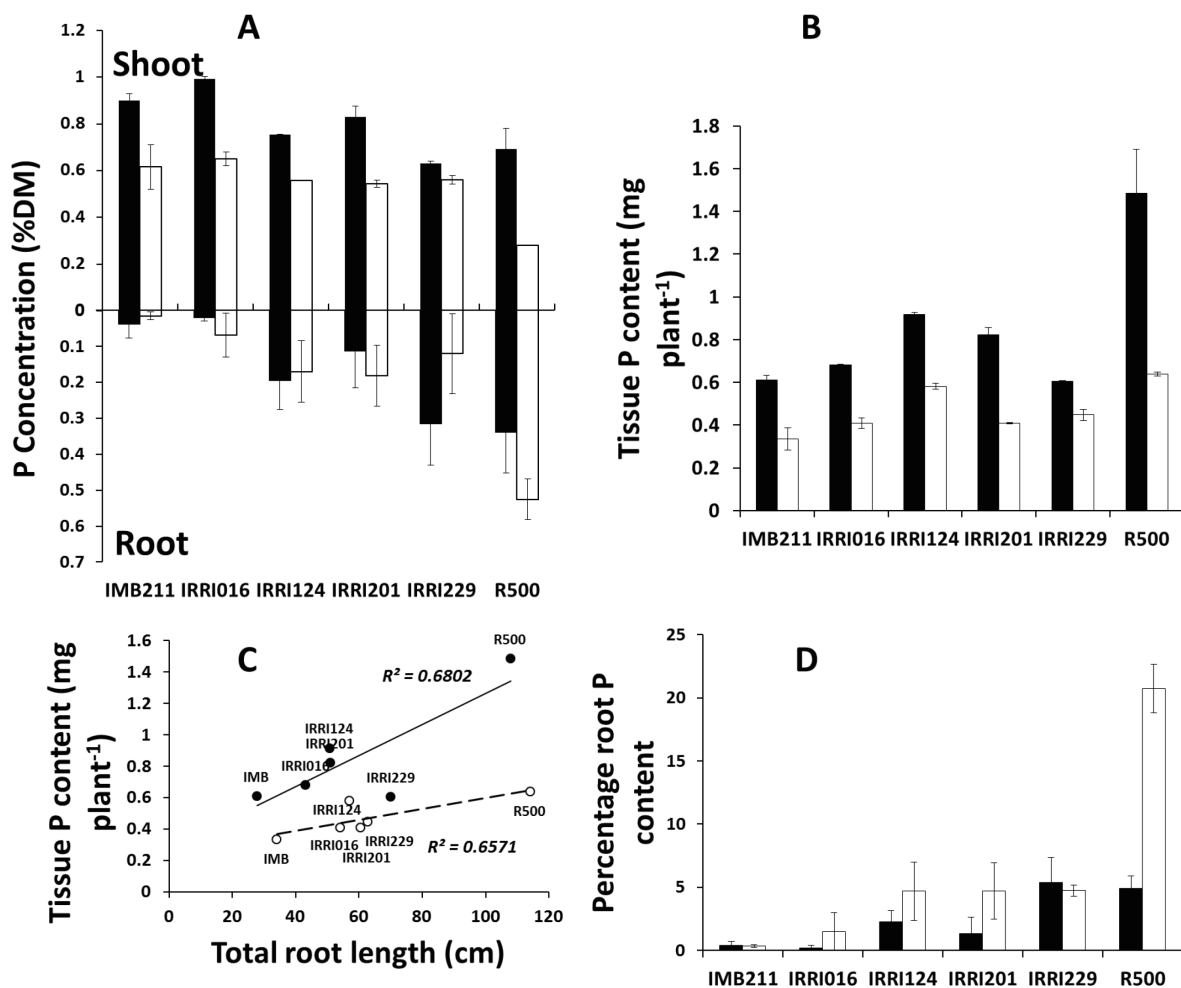


**Fig. 5.** Tissue Phosphorus (P) concentrations and its relationship with root systems of *Brassica rapa* genotypes grown for 21 DAS in soil-filled rhizoboxes amended with 0 (white columns) or 600  $\mu\text{M}$   $\text{KH}_2\text{PO}_4$  solution (black columns); Symbols represent means  $\pm$  s.e.m. ( $n = 12$ ). (A) P concentrations of shoot and roots; (B) P contents of the *Brassica rapa* genotypes; (C) Relationship between total root length (TRL) and plant P content. (D) Percentage partitioning of plant P content to roots.

RTD. Genotype  $\times$   $[P]_{\text{ext}}$  interactions accounted for variation ranging from 0 to 11% (Supplemental Table S3). Relatively consistent with the results of Experiment 1, and not surprising given the lack of  $G \times P$  interactions, broad-sense heritability ( $\sigma_g^2/\sigma_p^2$ ) was greatest for shoot biomass, number of LRs ( $>0.75$ ), RDW, surface area and TLRL ( $>0.60$ ). Broad-sense heritability was intermediate for TRL, PRL and mean LRL ( $>0.40$ ), but low ( $<0.40$ ) for the remaining traits (Supplemental Table S3). Whilst Run accounted for little variability (0–23%) in most traits, it accounted for 36, 64 and 99% of the variation in average diameter, branching density, and root angle, respectively (Supplemental Table S3).

#### *Tissue P concentration and P-content*

Increased P availability resulted in a large increase in  $[P]_{\text{shoot}}$  in all genotypes ( $P < 0.001$ , Fig. 5A). Tissue P content increased with increasing P supply (Fig. 5B). Total root length was strongly correlated with tissue P content both in plants grown on low  $[P]_{\text{ext}}$  soils ( $r = 0.81$ ,  $P < 0.05$ ; Fig. 5C) and on high  $[P]_{\text{ext}}$  soils ( $r = 0.82$ ,  $P < 0.05$ ; Fig. 5C). There was no consistent effect of P availability on  $[P]_{\text{root}}$  (Fig. 5A). However, four genotypes grown on un-amended soil IRR1016, IRR1124, IRR1201 and R500, partitioned 87%, 52%, 72% and 76% more P to their roots than their counterparts grown on soil amended with solution of 600  $\mu\text{M}$   $\text{KH}_2\text{PO}_4$ , respectively (Fig. 5D). The remaining two genotypes, IMB211 and IRR1229, partitioned 20% and 14% less P to the roots of plants grown on low  $[P]_{\text{ext}}$  soils than those grown on high  $[P]_{\text{ext}}$  soil, respectively (Fig. 5D).

#### *Relationship of tissue P concentration, seed P concentration and seed weight*

The mean seed P concentration of the six genotypes used in Experiment 2 were ranked in the order: R500 (1.12% DW)  $>$  IRR1124 (0.70% DW)  $>$  IMB211 (0.64% DW)  $>$  IRR1229 (0.62% DW)  $>$  IRR1201 (0.6% DW)  $>$  IRR1016 (0.58% DW). The contribution of seed P concentration to tissue P (shoot and root P) under high  $[P]_{\text{ext}}$  was low given that there was no significant relationship between seed P concentration and shoot P ( $r = 0.24$ ,  $P = 0.15$ ) and root P ( $r = 0.24$ ,  $P = 0.10$ ) at high  $[P]_{\text{ext}}$  (Supplemental Fig. S3A, S3B). Seed P concentration and tissue P concentration were correlated only at low  $[P]_{\text{ext}}$ . There was a significant relationship between seed P concentration and shoot P concentration ( $r = 0.84$ ,  $P < 0.01$ ) and root P concentration ( $r = 0.80$ ,  $P < 0.01$ ) at low  $[P]_{\text{ext}}$  (Supplemental Fig. S3A, S3B). The data revealed an

exponential (Seed P vs. Shoot P) and quadratic (Seed P vs. Root P) relationships for the best fit lines (Supplemental Fig. 3). Increase in seed P concentration from approximately 0.5% DM to 1.1% DM led to an exponential decrease in shoot P concentration from approximately 0.7% DM to 0.3% DM (Supplemental Fig. S3A, S3B). Increase in seed P concentration from approximately 0.5% DM to 0.7% DM led to a decrease in root P concentration from approximately 0.1% DM to 0.02% DM but root P concentration increased from approximately 0.04 to 0.6% DM when seed P concentrations were between 0.7 and 1.12% DM (Supplemental Fig. S3A, S3B). At high  $[P]_{\text{ext}}$ , shoot- and root P concentration showed a significant negative quadratic ( $r = 0.60$ ,  $P < 0.05$ ) and positive quadratic ( $r = 0.68$ ,  $P < 0.05$ ) correlation with seed mass, respectively (Supplemental Fig. S3C, S6D). The curvilinear correlations peaked at the seed mass of approximately 18 mg (per 10 seeds) for both shoot and root. Similarly, at low  $[P]_{\text{ext}}$ , shoot P and root P showed a significant negative quadratic ( $r = 0.63$ ,  $P < 0.05$ ) and positive quadratic ( $r = 0.61$ ,  $P < 0.05$ ) relationship with seed mass, respectively (Supplemental Fig. S3C, S3D). The curvilinear correlations peaked at the seed mass of 20 mg (per 10 seeds) and 12 mg (per 10 seeds) for shoot and root P, respectively (Supplemental Fig. S3C, S3D).

## **Discussion**

### *A simplified scanner-based, high resolution root imaging system*

In this study, a scanner-based phenotyping system on germination papers (Adu et al. 2014) was adopted to accommodate the imaging of roots grown in thin rhizoboxes following the design of Bengough et al. (2004). Results obtained in the present study suggest that a large proportion of the root system becomes visible on the transparent surface (Fig. 1). On average, the proportion of visible roots on the transparent surface of rhizoboxes and accessible for digitalisation was 85% (range: 78–93%). The slopes of the regression lines however changed depending on genotype (Fig. 2). This suggests that visible fraction of the root system may be a function of plant genotype and that total visible root length may not be a reliable indicator of actual root length in all cases. Generally, it seemed that the percentage of total visible roots might be related to specific root length (SRL) of a given genotype. Thus, roots that have a high length to dry mass ratio or SRL tended to position higher fraction of visible roots on the surface of the plate. For example, SRL was respectively, 37.7, 28.4 and 20.4  $\text{cm mg}^{-1}$  SDW for

the parental genotype IMB211, all the RILs combined and the parental genotype R500 and these correspondingly positioned on average 93, 84 and 86% of their actual total root system length along the surface of the transparent plate. It was also observed that PRs, which are larger and more gravitropic than LRs, were a major contributor to the TVRL and TRL (Table 2). The strong correlations between the TVRL and TRL (Fig. 1, 2) suggest that the use of thin rhizoboxes is an appropriate system to assess the TRL from TVRL for the genotypes studied. Our results agree with those of Nagel et al. (2012) who suggested that fraction of visible roots on rhizoboxes could be related to specific root weight.

Total root length (TRL) strongly correlated with root surface area but this was not surprising, given that this is a natural correlation where an increase in the PRL automatically increases the number of LR (and TLRL) and therefore TRL and root surface area. What was interesting was the significant positive correlation recorded between R:S and SRL. Specific root length is normally influenced by tissue density and strongly dependent on the fine root classes, (i.e. on roots <0.5 mm, <1 mm, <2 mm and 1–2 mm in diameter) (Wright and Westoby 1999, Ostonen et al. 2007, Paula and Pausas 2011). Whilst root biomass is a covariate for TRL and SRL considers individual variability in both TRL and root biomass, root dry mass fractions can mask shifts in root morphology or RSA by remaining constant when TRL increases or decreases with relatively small shifts in SRL (Paula and Pausas, 2011, Comas et al. 2013). Results here therefore suggest that root dry mass changed when TRL increased and this was accompanied with relatively small shifts in SRL. Strong phenotypic correlations observed between traits suggest that selection for a trait such as PR length will not be detrimental to other traits such as number of LR (Seiler 2008). However, in some cases, low correlation between traits may also be beneficial in permitting independent manipulation of traits (Gifford et al. 2013).

#### *Large replication is required to detect significant differences in RSA between genotypes*

The present study showed that CVs for many root traits are large with up to 40 replicates required to detect significant differences in root/shoot ratio between genotypes (Supplemental Table S1). Previously, the number of replications required to detect a significant difference in means of two genotypes using a 2-sided, 95% CI, *t*-test if trait means differed by 50% were estimated for seedlings

cultured on seed germination paper (Adu et al. 2014). Comparisons of the results of the present study with those of Adu et al. (2014) suggest that the growth environment influences the magnitude of variation in root traits and hence the replication required. For example, whilst 5 replicates, for TRL, and 20 replicates, for LRL, were estimated as adequate to detect a significant difference in means of two genotypes using a 2-sided, 95% CI, *t*-test if trait means differed by 50% when seedlings were grown in soil-filled rhizoboxes (Supplemental Table S1), 12 replicates for TRL and 14 replicates for LRL were estimated to be required to achieve the same statistical discrimination when seedlings were grown on paper (Adu et al. 2014).

#### *RSA traits of Brassica rapa seedlings exhibit temporal dynamics*

In the present study, it was observed that TRL increased sigmoidally for all genotypes in both runs (Supplemental Fig. S1). This occurrence must be put in context, given the relatively shorter duration for this experiment. Particularly for the genotypes with bigger root system size (e.g. R500 and IRR1380), it is possible that the plateauing of TRL is attributable to root growth restriction in the rhizoboxes. For example, in Fig. 1B, the LAUZ, which is a proxy for the average PR growth rate over the last ~100 hours (Lecompte et al. 2001), is much shorter on the plant with bigger root system than on the two others which do not reach the end of the rhizobox. This is visible on Fig. 4 where it is seen that PRL saturates at large values (with LAUZ decreasing, indicating restriction) while the LR number displays a progressive variation. In such situations and in the limits allowed by the variation of inter-lateral distance, the number of LR is probably a good substitute for PRL. Moreover, analysing root system growth with the assumption of a constant growth rate may be unrealistic (Paine et al. 2012, Adu et al. 2016). In the present study, analysis of root growth of a seedling through time showed that there were significant effects of both time and genotype on the dynamics of root growth (Table 2; Supplemental Fig. S1). Also, lateral root growth rate (LRGR) increased quadratically with time (DAS) for all genotypes (Supplemental Fig. S1) suggesting that if there was a restriction on PR growth, it did not apply to LR growth in the rhizobox.

One advantage of the logistic mixed-effects approach employed here to model aspects of RSA (Table 2; Supplemental Fig. S1) is that the behaviour of the model is biologically plausible (Calegario et al. 2005, Guan et al. 2006, Paine et al. 2012). The asymptote in the model may represent

root growth limitation due to changes in a seedlings' ontogeny, but under field conditions or studies of extended periods, it may also represent root growth limitation due to finite resources. The scale parameter indicates the time when root growth begins to slow down, perhaps due to growth restriction of bigger root systems in our system. Under field conditions, the scale parameter again may be reflecting limitation by finite resources or changes in a seedlings' ontogeny (Calegario et al. 2005, Guan et al. 2006, Paine et al. 2012). Such information could help identify root growth responses and stages of root development of seedlings. For example, genotypes with bigger asymptotes, but smaller inflection points and scale parameters, could suggest that growth was limited in the initial stages of seedling development. Thus, mixed-effects logistic modelling for example may answer biologically relevant questions such as the potential of different genotypes for early or sustained resource acquisition.

#### *Genotypic variation in seedling RSA traits and implications for phosphorus acquisition in Brassica rapa*

Variation in specific RSA traits and plasticity in response to P availability were observed among the genotypes studied (Fig. 3, Supplemental Fig. S2). In a similar study of oilseed rape (*Brassica napus* L.) grown in a rhizotron system, Yuan et al. (2016) reported that total root length and root tip number increased in high P than in low P plants and there was positive correlation between shoot and seed biomass with root biomass and other RSA traits at both high P than low P conditions. In the present study,  $[P]_{\text{ext}}$  did not alter PRL significantly, but it affected LAUZ significantly ( $P < 0.001$ ). Conclusions on this result must however be contextualised and cautiously drawn since, as alluded to earlier, it is possible that the effect on LAUZ reflects a restriction effect on PRL for genotypes with bigger root systems. In this study, effects of P on biomass and tissue P varied among different genotypes but genotypes varied in the extent of their responses to low P (Fig. 4). Based on theoretical considerations, significant genotypic variation in P concentration and P-content observed in the present study (Fig. 5) indicates the existence of useful genetic variation among genotypes for P-utilisation and P acquisition from environments with low P availability. The genetic variation observed between genotypes of *B. rapa* demonstrates the potential for breeding cultivars with improved P use efficiency, which will ultimately utilize applied inorganic Pi fertilizers

more efficiently (Hammond et al. 2009).

Shoot P concentration was significantly reduced in the parental genotype R500 at low  $[P]_{\text{ext}}$  (Fig. 5A). Given that shoot P content is a measure of P acquisition efficiency (Ozturk et al. 2005), it would seem that the rest of the genotypes were superior in P acquisition than the R500. However root P, percentage root P content and total tissue P were significantly higher in R500 at low  $[P]_{\text{ext}}$ , although total tissue P of IRR124 was comparable to that of R500 (Fig. 5). This result suggests that R500 was efficient at P acquisition but perhaps had a relatively reduced translocation of P to the shoot. Among the RILs, the results show that IRR124 was more P-efficient because it accumulated the highest DW among the RILs and also obtained the most tissue P at low  $[P]_{\text{ext}}$  (Fig. 4C, 5B). Therefore, the larger shoot biomass of the seedlings of the parental genotype R500 and IRR124 (among the RILs) indicated an increase in total P uptake.

For all genotypes, root length and tissue P content was highly correlated (Fig. 5C). It would, therefore, appear that P acquisition was limited in plants with reduced root system length and that the ability of roots to explore the soil volume was of greater importance for P acquisition than the rate of P uptake per unit root length. This is in agreement with many previous studies (Lynch 2007, White et al. 2012, White et al. 2013a, b). In the present study, a relative increase of partitioning of P to roots was shown to be a characteristic of *B. rapa* plants grown under a low  $[P]_{\text{ext}}$  regime. Under P deficient conditions, roots, the organs involved in P acquisition, lack P for growth and so will retain more P. Less P is consequently translocated to the shoot, generally leading to a reduced recycling of P from shoot to root. This acclimatory response of altered carbohydrate metabolism in shoots and attendant increased root-to-shoot (R:S) biomass ratio under P starvation has been reported (Hermans et al. 2006).

As seed P concentration can affect plant performance under P-deficient conditions (Ozturk et al. 2005), the seeds of the genotypes used in the present study were also analysed for P concentration and seed mass. It has been suggested by White and Veneklaas (2012) that seeds of crop plants generally contain P reserves to support maximal growth of seedlings for several weeks after germination. This allows the development of an extensive root system, required for the acquisition of P for continued growth. It was necessary to determine if the effect of  $[P]_{\text{ext}}$  on the brassica genotypes were confounded by internal seed P reserves considering the fact that the experiment lasted only 21 days. In the present study, the contribution of seed P concentration to tissue P

under high  $[P]_{\text{ext}}$  was low (Supplemental Fig. S3). Seed P concentration and tissue P concentration were correlated only at low  $[P]_{\text{ext}}$  (Supplemental Fig. S3). These results suggest that genotypic variation for tissue P at high  $[P]_{\text{ext}}$  is inherent or based on external P application and not related to seed P concentration. Genotypic variation for tissue P at low  $[P]_{\text{ext}}$  could however be confounded by seed P reserves. Thus, the effect of seed P on tissue P and by extension, P efficiency, may be greatest when there is a low external P supply. Consequently, seed P is not likely to be a major factor when adequate or high levels of P are applied. The results also indicate that tissue P concentration at low  $[P]_{\text{ext}}$  but not at high  $[P]_{\text{ext}}$  supply may be reliable parameter in ranking genotypes for P efficiency at the seedling stage of growth.

At both  $[P]_{\text{ext}}$  regimes, tissue P concentration showed a significant correlation with seed mass but the quadratic relationship was negative for shoot P and positive for root P (Supplemental Fig. S3). Liao and Yan (1999) reported similar results and suggested that increased seed mass enhances seed reserves for higher growth rate in seedlings leading to higher biomass produced per unit P absorbed. The authors also suggested that increased seed mass may increase cell size in leaf tissue in plants leading to greater leaf expansion for higher photosynthesis rate per unit P. The results of the present study indicate that variations in seed mass may have contributed to the variation in tissue P at the seedling stage for Brassica genotypes. Whist rhizobox setups might be useful in the detecting RSA response to varied  $[P]_{\text{ext}}$  levels; it is likely that variation in seed mass might confound effects of external P application at the early stages of plant growth. At the seedling stage, higher seed weight may contribute to higher tissue P, and therefore, should be considered in evaluation of genotypes for P efficiency.

## Conclusions

The results presented in this study show that about 85% of the root system of seedlings can be observed in a scanner-based, soil-filled rhizobox system. Soil-filled rhizobox systems can provide information on genotypic and environmental effects on RSA provided an appropriate number of replicates are used. Seed P concentration and tissue P concentration were correlated only at low  $[P]_{\text{ext}}$ , suggesting that genotypic variation for tissue P at high  $[P]_{\text{ext}}$  is inherent or based on external P application and not related to seed P concentration. It was also found that, at the seedling stage, higher seed weight may contribute to higher tissue P, and therefore, should be considered in evaluation of

genotypes for P efficiency. The results of the P supply experiment demonstrate the potential for using this system to quantify environmental and temporal variations in traits contributing to RSA provided the confounding effects of seed P reserves and seed weight especially at low  $[P]_{\text{ext}}$  can be delineated.

## Acknowledgements

This work was supported by the Rural and Environment Science and Analytical Services Division (RESAS) of the Scottish Government through Work Package 3.3, 'The soil, water and air interface and its response to climate and land use change' (2011-2016). Funding for this study was provided in part by the UK Biotechnology and Biological Sciences Research Council (BBSRC) Crop Improvement Research Club (grant BB/J019631/1) and a BBSRC Professorial Fellowship (to M.J.B.). M.O.A. was supported by the University of Nottingham Vice-Chancellor's Scholarship for Research Excellence. Tim George, Lawrie Brown, Glyn Bengough and Ken Loades provided invaluable help in the provision of soil and rhizoboxes. The authors are grateful for advice from Jim McNichol and Christine Hackett on the statistical analyses.

## References

- Adu MO, Chatot A, Wiesel L, Bennett MJ, Broadley MR, White PJ, Dupuy LX 2014 A scanner system for high-resolution quantification of variation in root growth dynamics of *Brassica rapa* genotypes. *J. Exp. Bot.* 65: 2039-2048.
- Adu MO, Wiesel L, Bennett MJ, Broadley MR, White PJ, Dupuy LX 2015 Scanner-based time-lapse root phenotyping. *Bio-protocol* 5: e1424.
- Adu MO, Yawson DO, Armah FA, Asare PA, Bennett MJ, Broadley MR, White PJ, Dupuy LX 2016 Effects of rooting media on root growth and morphology of *Brassica rapa* seedlings. *S. Afr. J. Plant Soil* 33: 219-227.
- Asseng S, Aylmore LAB, MacFall JS, Hopmans JW, Gregory PJ 2000 Computer-assisted tomography and magnetic resonance imaging. In: Smit AL, Bengough AG, Engels C, van Noordwijk M, Pellerin S, van de Geijn SC, eds., *Root methods: a handbook*. Springer, Heidelberg, Germany, pp. 343-363.
- Bengough AG, Gordon DC, Al-Menaie H, Ellis RP, Allan D, Keith R, Thomas WTB, Forster BP. 2004 Gel observation chamber for rapid screening of root traits in cereal seedlings. *Plant Soil* 262: 63-70.
- Brown LK, George TS, Thompson JA, Wright G, Lyon J, Dupuy L, Hubbard SF, White PJ 2012 What are the implications of variation in root hair length on tolerance to phosphorus deficiency in combination with water stress in barley (*Hordeum vulgare*)? *Ann. Bot.* 110: 319-328.

- Calegario N, Daniels RF, Maestri R, Neiva R 2005 Modeling dominant height growth based on nonlinear mixed-effects model: a clonal eucalyptus plantation case study. *Forest Ecol. Manag.* 204: 11-21.
- Comas LH, Becker SR, Cruz VM, Byrne, PF, Dierig DA 2013 Root traits contributing to plant productivity under drought. *Front. Plant Sci.* 4:442.
- Crush JR, Care DA, Gourdin A, Woodfield DR 2005 Root growth media effects on root morphology and architecture in white clover. *New Zeal. J. Agr. Res.* 48: 255-263.
- Dai X, Wang Y, Yang A, Zhang WH 2012 *OsMYB2P-1*, an R2R3 MYB transcription factor, is involved in the regulation of phosphate-starvation responses and root architecture in rice. *Plant Physiol.* 159: 169-183.
- Downie HF, Adu MO, Schmidt S, Otten W, Dupuy LX, White PJ, Valentine TA 2015 Challenges and opportunities for quantifying roots and rhizosphere interactions through imaging and image analysis. *Plant Cell Environ.* 38: 1213-1232.
- Dupuy L, Gregory PJ, Bengough AG 2010a Root growth models: towards a new generation of continuous approaches. *J. Exp. Bot.* 61: 2131-2143.
- Dupuy L, Vignes M, McKenzie BM, White PJ 2010b The dynamics of root meristem distribution in the soil. *Plant Cell Environ.* 33: 358-369.
- Faget M, Nagel KA, Walter A, Herrera JM, Jahnke S, Schurr U, Temperton VM 2013 Root-root interactions: extending our perspective to be more inclusive of the range of theories in ecology and agriculture using *in-vivo* analyses. *Ann. Bot.* 112: 253-266.
- Galkovskiy T, Mileyko Y, Bucksch A, Moore B, Symonova O, Price C, Topp C, Iyer-Pascuzzi A, Zurek P, Fang S, Harer J, Benfey P, Weitz J 2012 GiA Roots: software for the high throughput analysis of plant root system architecture. *BMC Plant Biol.* 12: 116.
- Garrigues E, Doussan C, Pierret A 2006 Water uptake by plant roots: I - Formation and propagation of a water extraction front in mature root systems as evidenced by 2D light transmission imaging. *Plant Soil* 283: 83-98.
- George TS, Brown LK, Newton AC, Hallett PD, Sun BH, Thomas WTB, White PJ 2011 Impact of soil tillage on the robustness of the genetic component of variation in phosphorus (P) use efficiency in barley (*Hordeum vulgare* L.). *Plant Soil* 339: 113-123.
- Ghanem ME, Hichri I, Smigoeki AC, Albacete A, Fauconnier ML, Diatloff E, Martinez-Andujar C, Lutts S, Dodd IC, Perez-Alfocea F 2011 Root-targeted biotechnology to mediate hormonal signalling and improve crop stress tolerance. *Plant Cell Rep.* 30: 807-823.
- Gifford ML, Banta JA, Katari MS, Hulsmans J, Chen L, Ristova D, Tranchina D, Purugganan MD, Coruzzi GM, Birnbaum KD 2013 Plasticity regulators modulate specific root traits in discrete nitrogen environments. *PLOS Genet.* 9: e1003760.
- Gregory PJ 2006 *Plant roots: their growth, activity and interaction with soils.* Blackwell Publishing, Oxford, UK, pp. 45-64.
- Gregory PJ, Bengough AG, Grinev D, Schmidt S, Thomas WTB, Wojciechowski T, Young IM 2009 Root phenomics of crops: opportunities and challenges. *Funct. Plant Biol.* 36: 922-929.
- Gruber BD, Giehl RFH, Friedel S, von Wirén N 2013 Plasticity of the *Arabidopsis* root system under nutrient deficiencies. *Plant Physiol.* 163: 161-179.
- Guan BT, Chang TY, Shih PC, Lin ST 2006 Application of a nonlinear mixed-effects model to assess the effects of nursery nitrogen fertilization on seedling height growth of Taiwan yellow false cypress. *Taiwan J. For. Sci.* 21: 67-74.
- Hammond JP, Broadley MR, White PJ, King GJ, Bowen HC, Hayden R, Meacham MC, Mead A, Overs T, Spracklen WP, Greenwood DJ 2009 Shoot yield drives phosphorus use efficiency in *Brassica oleracea* and correlates with root architecture traits. *J. Exp. Bot.* 60: 1953-1968.
- Hermans C, Hammond JP, White PJ, Verbruggen N 2006 How do plants respond to nutrient shortage by biomass allocation? *Trends Plant Sci.* 11: 610-617.
- Hodge A, Robinson D, Griffiths BS, Fitter AH 1999 Why plants bother: root proliferation results in increased nitrogen capture from an organic patch when two grasses compete. *Plant Cell Environ.* 22: 811-820.
- Hund A, Trachsel S, Stamp P 2009 Growth of axile and lateral roots of maize: I development of a phenotyping platform. *Plant Soil* 325: 335-349.
- Hutchings MJ, John EA 2004 The effects of environmental heterogeneity on root growth and root/shoot partitioning. *Ann. Bot.* 94: 1-8.
- Iniguez-Luy FL, Lukens L, Farnham MW, Amasino RM, Osborn TC 2009 Development of public immortal mapping populations, molecular markers and linkage maps for rapid cycling *Brassica rapa* and *B. oleracea*. *Theor. Appl. Genet.* 120: 31-43.
- Irving GCJ, McLaughlin MJ 1990 A rapid and simple field-test for phosphorus in Olsen and Bray No 1 extracts of soil. *Commun. Soil Sci. Plant Anal.* 21: 2245-2255.
- Iyer-Pascuzzi AS, Symonova O, Mileyko Y, Hao YL, Belcher H, Harer J, Weitz JS, Benfey PN 2010 Imaging and analysis platform for automatic phenotyping and trait ranking of plant root systems. *Plant Physiol.* 152: 1148-1157.
- Jain A, Poling MD, Smith AP, Nagarajan VK, Lahner B, Meagher RB, Raghothama KG 2009 Variations in the composition of gelling agents affect morphophysiological and molecular responses to deficiencies of phosphate and other nutrients. *Plant Physiol.* 150: 1033-1049.
- Kalogiros DI, Adu MO, White PJ, Broadley MR, Draye X, Ptashnyk M, Bengough AG, Dupuy LX 2016 Analysis of root growth from a phenotyping dataset using a density-based model. *J. Exp. Bot.* 67: 1045-1058.
- Kim K-R, Owens G, Kwon S-I 2010 Influence of Indian mustard (*Brassica juncea*) on rhizosphere soil solution chemistry in long-term contaminated soils: A rhizobox study. *J. Environ. Sci.* 22: 98-105.
- Kosola KR, Workmaster BAA, Busse JS, Gilman JH 2007 Sampling damage to tree fine roots: comparing air excavation and hydropneumatic elutriation. *HortScience* 42: 728-731.
- Lecompte F, Ozier-Lafontaine H, Pages L 2001 The relationships between static and dynamic variables in the



- description of root growth. Consequences for field interpretation of rooting variability. *Plant Soil* 236: 19-31.
- LeMarié C, Kirchgessner N, Marschall D, Walter A, Andreas H 2014 Rhizoslides: paper-based growth system for non-destructive, high throughput phenotyping of root development by means of image analysis. *Plant Method.* 10: 13.
- Liao H, Rubio G, Yan XL, Cao AQ, Brown KM, Lynch JP 2001 Effect of phosphorus availability on basal root shallowness in common bean. *Plant Soil* 232: 69-79.
- Liao H, Yan X 1999 Seed size is closely related to phosphorus use efficiency and photosynthetic phosphorus use efficiency in common bean. *J. Plant Nutr.* 22: 877-888.
- Lobet G, Pagès L, Draye X 2011 A novel image-analysis toolbox enabling quantitative analysis of root system architecture. *Plant Physiol.* 157: 29-39.
- Lynch JP 2007 Roots of the second green revolution. *Aust. J. Bot.* 55: 493-512.
- Mairhofer S, Zappala S, Tracy SR, Sturrock C, Bennett M, Mooney SJ, Pridmore TP 2013 Recovering complete plant root system architectures from soil via X-ray  $\mu$ -computed tomography. *Plant Method.* 9: 8.
- Moradi A, Conesa H, Robinson B, Lehmann E, Kuehne G, Kaestner A, Oswald S, Schulin R. 2009 Neutron radiography as a tool for revealing root development in soil: capabilities and limitations. *Plant Soil* 318: 243-255.
- Nagel KA, Kastenholz B, Jahnke S, Van Dusschoten D, Aach T, Muhlich M, Truhn D, Scharr H, Terjung S, Walter A, Schurr U 2009 Temperature responses of roots: impact on growth, root system architecture and implications for phenotyping. *Funct. Plant. Bio.* 36: 947-959.
- Nagel KA, Putz A, Gilmer F, Heinz K, Fischbach A, Pfeifer J, Faget M, Blossfeld S, Ernst M, Dimaki C, Kastenholz B, Kleinert AK, Galinski A, Scharr H, Fiorani F, Schurr U 2012 GROWSCREEN-Rhizo is a novel phenotyping robot enabling simultaneous measurements of root and shoot growth for plants grown in soil-filled rhizotrons. *Funct. Plant Biol.* 39: 891-904.
- Neumann G, George TS, Plassard C 2009 Strategies and methods for studying the rhizosphere - the plant science toolbox. *Plant Soil* 321: 431-456.
- Ostonen I, Püttsepp Ü, Biel C, Alberton, O, Bakker MR, Löhmus K, Brunner I 2007 Specific root length as an indicator of environmental change. *Plant Biosyst.* 14: 426-442.
- Ozturk L, Eker S, Torun B, Cakmak I 2005 Variation in phosphorus efficiency among 73 bread and durum wheat genotypes grown in a phosphorus-deficient calcareous soil. *Plant Soil* 269: 69-80.
- Paine CET, Marthens TR, Vogt DR, Purves D, Rees M, Hector A, Turnbull LA 2012 How to fit nonlinear plant growth models and calculate growth rates: an update for ecologists. *Method. Ecol. Evol.* 3: 245-256.
- Paula S, Pausas JG 2011 Root traits explain different foraging strategies between resprouting life histories. *Oecologia* 165: 321-331.
- Perret JS, Al-Belushi ME, Deadman M 2007 Non-destructive visualization and quantification of roots using computed tomography. *Soil Biol. Biochem.* 39: 391-399.
- Pinheiro J, Bates D, DebRoy S, Sarkar D, Team. TRC 2008 nlme: Linear and Nonlinear Mixed Effects Models. R package version 3.1- 89.
- Pinheiro JC, Bates DM 2000 Mixed-Effects Models in S and S-PLUS. Springer, New York, pp. 271-409.
- Seiler GJ. 2008 Root growth of interspecific sunflower seedlings derived from wild perennial sunflower species. *Can. J. Plant Sci.* 88: 705-712.
- Shi L, Shi T, Broadley MR, White PJ, Long Y, Meng J, Xu F, Hammond JP 2013 High-throughput root phenotyping screens identify genetic loci associated with root architectural traits in *Brassica napus* under contrasting phosphate availabilities. *Ann. Bot.* 112 : 381-389.
- Soledad GN, Salazar MJ, Pignata ML, Rodriguez JH 2016 Assessment of the root system of *Brassica juncea* (L.) Czern. and *Bidens pilosa* L. exposed to lead polluted soils using rhizobox systems. *Int. J. Phytoremediat.* 18: 235-44.
- Thomas CL, Graham NS, Hayden R, Meacham MC, Neugebauer K, Nightingale M, Dupuy LX, Hammond JP, White PJ, Broadley MR 2016 High throughput phenotyping (HTP) identifies seedling root traits linked to variation in seed yield and nutrient capture in field-grown oilseed rape (*Brassica napus* L.). *Ann. Bot.* 118: 655-665.
- Tracy SR, Roberts JA, Black CR, McNeill A, Davidson R, Mooney SJ 2010 The X-factor: visualizing undisturbed root architecture in soils using X-ray computed tomography. *J. Exp. Bot.* 61: 311-313.
- van Noordwijk M, Brouwer G, Meijboom F, Oliveira MDRG, Bengough AG 2000 Trench profile techniques and core break methods. In: Smit AL, Bengough AG, Engels C, van Noordwijk M, Pellerin S, van de Geijn SC, Eds. *Root methods: a handbook*. Springer, Heidelberg, Germany, pp. 211-233.
- White PJ, Broadley MR, Gregory PJ 2012 Managing the nutrition of plants and people. *Appl. Environ. Soil Sci.* 2012: Article ID 104826.
- White PJ, George TS, Dupuy LX, Karley AJ, Valentine TA, Wiesel L, Wishart J 2013a Root traits for infertile soils. *Front. Plant Sci.* 4: 193.
- White PJ, George TS, Gregory PJ, Bengough AG, Hallett PD, McKenzie BM 2013b Matching roots to their environment. *Ann. Bot.* 112: 207-222.
- White PJ, Veneklaas EJ 2012 Nature and nurture: the importance of seed phosphorus content. *Plant Soil* 357: 1-8.
- Wright IJ, Westoby M 1999 Differences in seedling growth behaviour among species: trait correlations across species, and trait shifts along nutrient compared to rainfall gradients. *J. Ecol.* 87: 85-97.
- Xu XD, Xie QG, McClung CR 2010 Robust circadian rhythms of gene expression in *Brassica rapa* tissue culture. *Plant Physiol.* 153: 841-850.
- Yazdanbakhsh N, Fisahn J 2012 High-throughput phenotyping of root growth dynamics. *Methods Mol. Biol.* 918: 21-40.
- Yuan P, Ding GD, Cai HM, Jin KM, Broadley MR, Xu FS, Shi L 2016 A novel *Brassica* rhizotron system to unravel the dynamic changes in root system architecture of oilseed rape under phosphorus deficiency. *Ann. Bot.* 118: 173-184.

**Supplemental Table S1**, Descriptive statistics for traits measured on the parents and 10 RIL of *Brassica rapa* L. seedlings grown for 15 days after transfer to soil-filled rhizoboxes

Traita	Unit	Descriptive statistics for all genotypes				Difference between means of parental lines	SD's	Estimated sample size <sup>ii</sup>
		Minimum	Maximum	Mean	CV (%)			
SFW	mg	24	333.3	111.07	43.02	144.4	45.4	12
SDW	mg	1.1	16.6	5.64	38.39	6.21	2.38	18
RFW	mg	3.5	39.5	13.75	43.18	19.91	4.84	7
RDW	mg	0.1	4.4	1.05	63.54	2.24	0.57	8
TRL	cm	4.27	77.27	28.32	47.73	40.84	11.6	10
TLRL	cm	1.42	64.59	16.84	57.69	27	8.89	14
PRL	cm	4.69	28.7	13.93	30.23	14.65	3.17	6
B. Dens.	root cm <sup>-1</sup>	0.59	3.89	1.71	32.39	0.24	0.52	590
NLR	-	2	34	12.59	51.18	19.75	3.54	4
LRL	cm	0.08	1.93	0.68	43.11	0.32	0.18	39
Angle	°	55.53	94.82	67.33	9.46	1.86	7.82	2212
Int. Dist.	cm	0.3	3.01	0.8	47.14	0.11	0.26	762
Mean Diam.	mm	0.25	0.42	0.31	10.64	2.81	1.22	24
Surf. Area	cm <sup>2</sup>	2.57	8.84	6.77	19.02	28.75	11.7	21
Root Vol.	mm <sup>3</sup>	4	64	20.89	55.25	0	-	-
LAUZ	cm	2.48	18.99	6.15	37.89	4.03	2.25	39
R:S	-	0.03	0.72	0.19	53.2	0.21	0.13	48
SRL	cm mg <sup>-1</sup>	8.48	94.45	32.68	53.11	19.79	19	116

<sup>a</sup>Abbreviations: Shoot Fresh Weight (SFW), Shoot Dry Weight (SDW), Root Fresh Weight (RFW), Root Dry Weight (RDW), Total Root Length (TRL), Total Lateral Root Length (TLRL), Primary Root Length (PRL), Branching Density (B. Dens.), Number of Lateral Roots (NLR), Mean Lateral Root Length (LRL), Root Insertion Angle (Angle), Lateral Root Interbranch Distance (Int. Dist.), Mean Root Diameter (Mean Diam.), Total Surface Area of Root (Surf. Area), Root Volume (Root Vol.), Length of the Primary Root Apical Unbranched Zone (LAUZ), RDW/SDW (R:S), Specific Root Length (SRL).

Sample size was estimated based on the difference between mean values of the parental genotypes for each trait. CV: Coefficient of variation, <sup>i</sup>SD: standard deviation - estimated as 50% of the sum of SDs calculated for a given trait for each parent;

<sup>ii</sup>represents the sum of the estimated sample size for both parental genotypes and calculated for 50% difference between means.

**Supplemental Table S2.** Genotypic variation in shoot and root traits assayed 15 DAS among the parents (IMB211, R500) and 10 RILs of the *Brassica rapa* L. of the BraIRRI mapping population grown for 15 days in soil-filled rhizobox system (\*\*  $P < 0.001$  or \* $P < 0.005$ ,  $n = 12$  plants; d.f = 143; ns = Not Significant; LSD = Least Significant Difference)

Trait <sup>a</sup>	IMB211	IRRI002	IRRI016	IRRI030	IRRI104	RI124	IRRI198	IRRI201	IRRI229	IRRI360	IRRI380	R500	P	LSD
SFW	50.4	105.2	115.3	56.8	102.5	102.5	143.7	130.3	112.1	114	105	194.8	**	26.55
SDW	3	5.23	5.03	4.04	4.7	5.24	7.12	6.13	6.17	6.47	5.28	9.21	**	1.298
RFW	5.41	13.65	11.12	9.52	14.28	11.62	13.57	16.4	15.7	12.76	15.63	25.32	**	3.19
RDW	0.28	1	0.717	0.842	0.817	1.083	1.083	1.053	1.017	1.113	1.067	2.517	**	0.3716
TRL	10.55	30.32	24.09	20.9	28.7	24.81	28.89	34.03	31.5	27.67	26.94	51.39	**	8.415
Mean Diam.	0.306	0.296	0.315	0.3	0.318	0.315	0.312	0.298	0.296	0.328	0.323	0.307	ns	0.026
Surf. Area	4.811	7.276	6.85	6.408	7.338	6.66	6.628	6.846	7.018	6.577	7.205	7.62	**	0.9163
Root Vol.	8.14	20.9	18.25	15.25	22.92	19.58	22.25	22.52	22.42	19.18	22.33	36.92	**	8.115
PRL	7.35	14.25	12.76	10.67	15.71	12.28	14.1	15.07	14.04	14.33	14.6	22	**	2.217
B. Dens.	1.868	2.015	2.022	1.561	1.149	1.694	1.728	1.703	1.785	1.851	1.489	1.63	*	0.4227
LRN.	4.47	15.15	8.58	7.67	9.88	12	14.42	14.57	14.33	15.83	9.92	24.25	**	3.532
LRL	0.278	0.705	0.69	0.768	0.679	0.655	0.886	0.93	0.716	0.678	0.52	0.598	**	0.2038
Angle	71.09	69.69	68.09	69.6	69.79	64.26	62.56	65.76	65.97	66.05	65.86	69.23	*	4.919
Int. Dist.	0.853	0.581	0.791	0.841	1.409	0.711	0.695	0.665	0.628	0.668	1.038	0.746	**	0.2596
LAUZ	4.41	6.58	7.25	5.49	7.11	5.29	5.43	6.08	5.77	5.57	7.49	8.44	**	1.475
LBZ	4.31	18.56	12.03	11.08	14.73	14.96	21.15	23.15	18.88	19.48	12.46	31.31	**	5.975
SRL	43.8	34.2	43.7	26.4	40.8	24.2	30.7	32.1	31.5	32.4	28.4	24	*	13.48
R:S	0.1075	0.1891	0.1492	0.2244	0.1761	0.2192	0.1546	0.173	0.1694	0.1725	0.2142	0.3166	**	0.07332

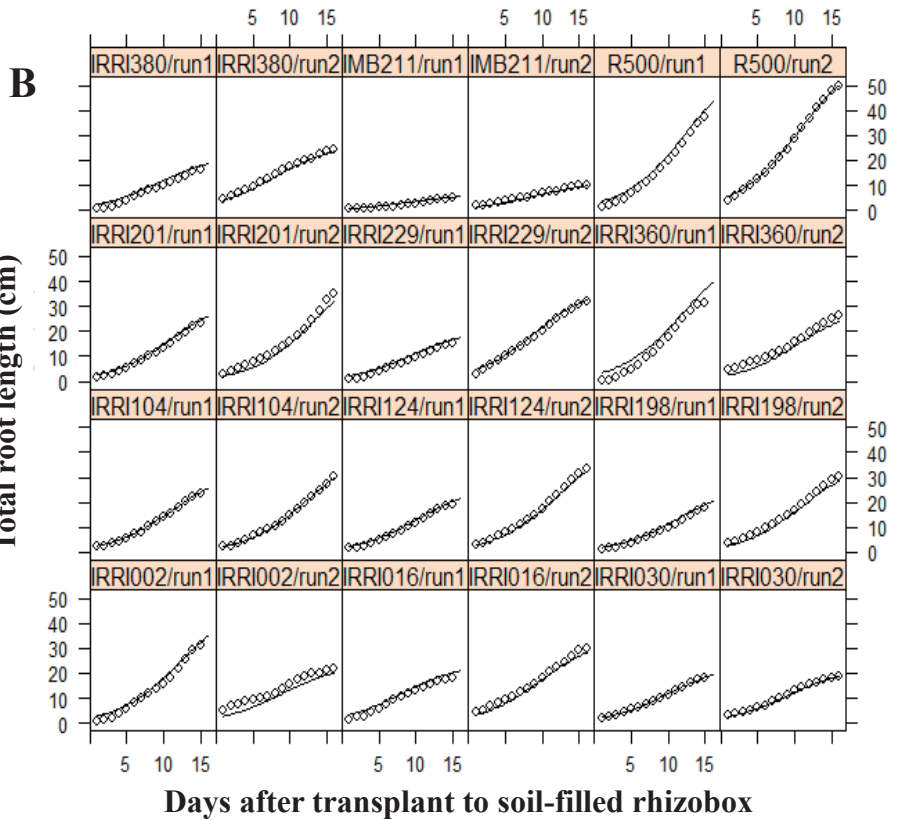
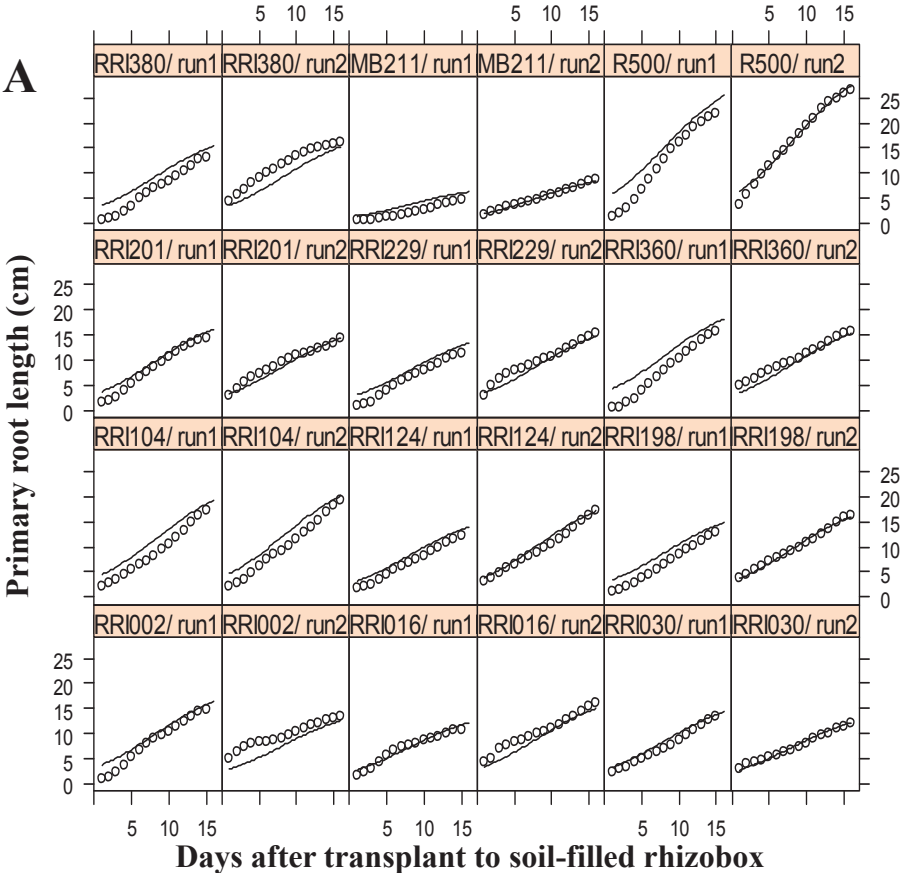
<sup>a</sup>Abbreviations: Shoot Fresh Weight (SFW), Shoot Dry Weight (SDW), Root Fresh Weight (RFW), Root Dry Weight (RDW), Total Root Length (TRL), Mean Root Diameter (Mean Diam.), Total Surface Area of Root (Surf. Area), Root Volume (Root Vol.), Primary Root Length (PRL), Branching Density (B. Dens.), Number of Lateral Roots (NLR), Mean Lateral Root Length (LRL), Root Insertion Angle (Angle), Lateral Root Interbranch Distance (Int. Dist.), Length of the Primary Root Apical Unbranched Zone (LAUZ), Length of the Branching Zone of the root system (LBZ), Specific Root Length (SRL), RDW/ SDW (R:S).

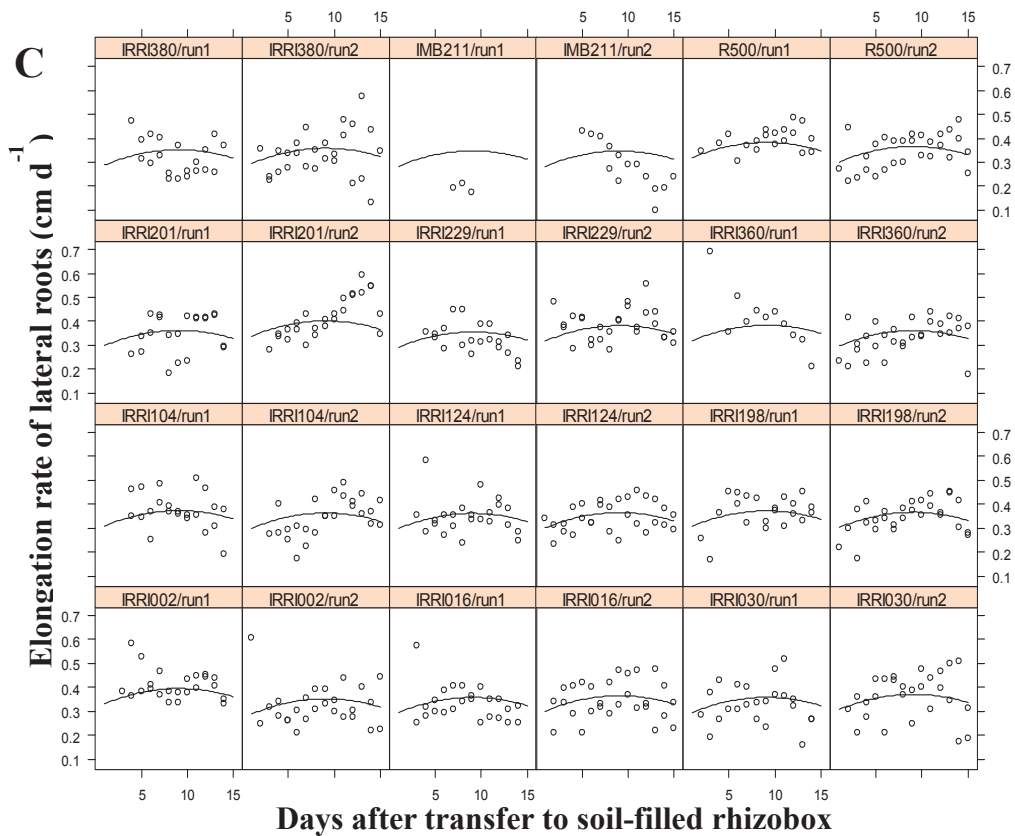
**Supplemental Table S3.** Sources of variation and broad sense heritability ( $H^2$ ) in shoot and root traits assayed among the parents and four recombinant inbred lines of the *Brassica rapa* BraIRRI mapping population grown in soil filled rhizoboxes at differential external P concentration for up to 21 days in the phenotyping platform

Trait <sup>a</sup>	Variances of effects						Source of variation (%)					
	$\mu$	$\sigma_g^2$	$\sigma_\beta^2$	$\sigma_a^2$	$\sigma_{ga}^2$	$\sigma_e^2$	$H^2$	Run	Genotype	[P] <sub>ext</sub>	Gen.×[P] <sub>ext</sub>	Residual
SFW (mg)	209	$14.2 \times 10^3$	5	83	20	$16.2 \times 10^2$	0.89	0	89	1	0	10
SDW (mg)	11.9	33.8	$3.8 \times 10^{-1}$	2	0	6.9	0.78	1	78	5	0	16
RFW (mg)	25.5	$2.5 \times 10^{-1}$	$1.3 \times 10^{-2}$	$7.4 \times 10^{-3}$	0	$2.1 \times 10^{-1}$	0.52	2.7	51.8	1.5	0	44
RDW (mg)	1.4	$5.5 \times 10^{-1}$	$3.9 \times 10^{-2}$	$3.1 \times 10^{-2}$	$1.2 \times 10^{-2}$	$2.3 \times 10^{-1}$	0.64	4.5	64	3.6	1.2	26.7
TRL (cm)	61.2	$72.2 \times 10$	$26.1 \times 10$	10.9	0	$30 \times 10$	0.56	20.2	55.8	0.8	0	23.2
TLRL (cm)	55.7	$80.1 \times 10$	$16.4 \times 10$	24.6	0	$29.1 \times 10$	0.63	12.8	62.5	2	0	22.7
PRL (cm)	21.4	23.61	$3 \times 10^{-2}$	$3.3 \times 10^{-1}$	0	$1.63 \times 10$	0.59	0.1	58.6	0.8	0	40.5
Mean Diam.(mm)	0.39	$2.1 \times 10^{-5}$	$10.3 \times 10^{-4}$	$5.4 \times 10^{-4}$	$11.4 \times 10^{-4}$	$11.3 \times 10^{-4}$	0.01	36.5	0.7	19	4	39.8
NLR	21.5	$10.7 \times 10^{-1}$	0	0	0	$33.6 \times 10^{-2}$	0.76	0	76	0	0	24
Angle (°)	69.2	$16.7 \times 10^{-5}$	$27.3 \times 10^{-1}$	0	$46.4 \times 10^{-5}$	$83.1 \times 10^{-4}$	0	99.7	0	0	0	0.3
Int. Dist. (cm)	1	$9.8 \times 10^{-3}$	0	0	$6.8 \times 10^{-3}$	$14.2 \times 10^{-2}$	0.06	0	6.2	0	4.3	89.5
Mean LRL (cm)	1.1	$12 \times 10^{-2}$	0	$7 \times 10^{-4}$	0	$14.2 \times 10^{-2}$	0.46	0	45.6	0.3	0	54.1
LAUZ (cm)	5.6	$43.4 \times 10^{-1}$	$7.7 \times 10^{-2}$	$13.8 \times 10^{-1}$	0	$8.7 \times 10^{-1}$	0.3	0	30	10	0	60
B. Dens. (root cm <sup>-1</sup> PRL)	1.6	$8 \times 10^{-5}$	$20.6 \times 10^{-2}$	$7.4 \times 10^{-2}$	0	$4.9 \times 10^{-2}$	0	62.5	0	22.5	0	15
R:S	0.12	$2.5 \times 10^{-5}$	$7 \times 10^{-6}$	$9.3 \times 10^{-4}$	$7.4 \times 10^{-5}$	$20.2 \times 10^{-4}$	0.01	0.2	0.8	30.4	2.4	66.2
Root vol. (cm <sup>3</sup> )	0.07	$7.3 \times 10^{-4}$	$8.4 \times 10^{-6}$	$4.7 \times 10^{-5}$	$13.1 \times 10^{-5}$	$5.4 \times 10^{-4}$	0.5	0.5	50	3.2	9	37.3
Surf. area (cm <sup>2</sup> )	7.3	$92.7 \times 10^{-1}$	$81.1 \times 10^{-2}$	0	$41.5 \times 10^{-2}$	$44.1 \times 10^{-1}$	0.62	5.4	62.2	0	2.9	29.5
Area: Vol. (cm <sup>-1</sup> )	104	$9 \times 10^{-1}$	58	43.3	13.8	131.7	0	23.4	0.4	17.5	5.5	53.2
RTD (RDW/Root fresh vol.; g cm <sup>-3</sup> )	0.02	$1.2 \times 10^{-5}$	$8.1 \times 10^{-6}$	$2.0 \times 10^{-5}$	$1.2 \times 10^{-5}$	$5.7 \times 10^{-5}$	0.11	7.4	11.2	18.5	11.1	51.8

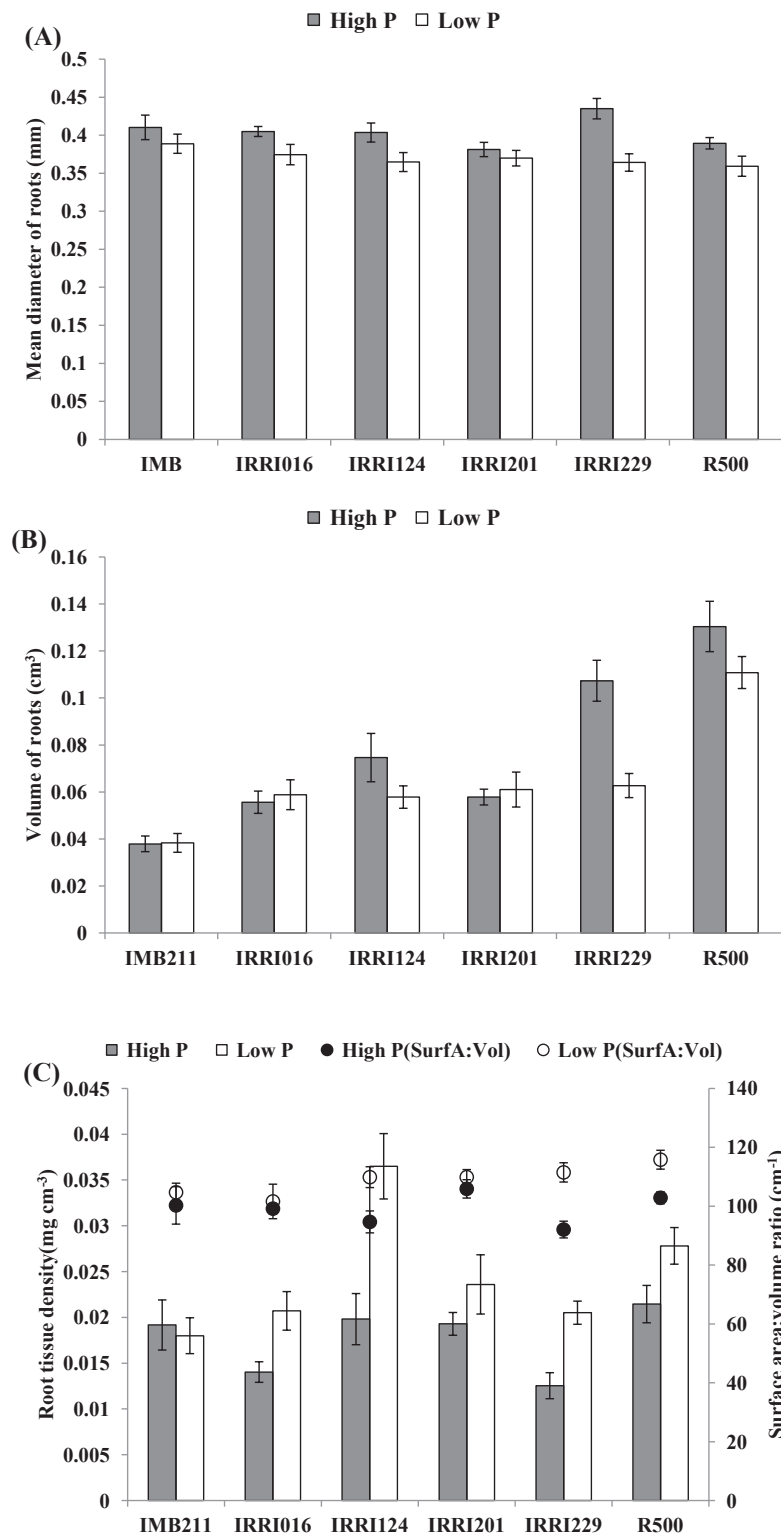
<sup>a</sup>Abbreviations: Shoot Fresh Weight (SFW), Shoot Dry Weight (SDW), Root Fresh Weight (RFW), Root Dry Weight (RDW), Total Root Length (TRL), Total Lateral Root Length (TLRL), Primary Root Length (PRL), Mean Root Diameter (Mean Diam.), Number of Lateral Roots (NLR), Root Insertion Angle (Angle), Lateral Root Interbranch Distance (Int. Dist.), Mean Lateral Root Length (LRL), Length of the Primary Root Apical Unbranched Zone (LAUZ), Branching Density (B. Dens.), RDW/ SDW (R:S). Total Root Volume (Root Vol.), Total Surface Area of Root (Surf. Area), Total root volume / Total root area (Area:Vol.), Root Tissue Density (RTD).

$\mu$  = the overall mean,  $\sigma_g^2$  = estimated variance associated with the effect of genotype,  $\sigma_\beta^2$  = estimated variance associated with the effect of experimental run,  $\sigma_a^2$  = estimated variance associated with the effect of external phosphorus concentration,  $\sigma_{ga}^2$  = estimated covariance associated with the effect of genotype x external phosphorus concentration,  $\sigma_e^2$  = estimated variance associated with the residual error,  $H^2$  = broad-sense heritability.

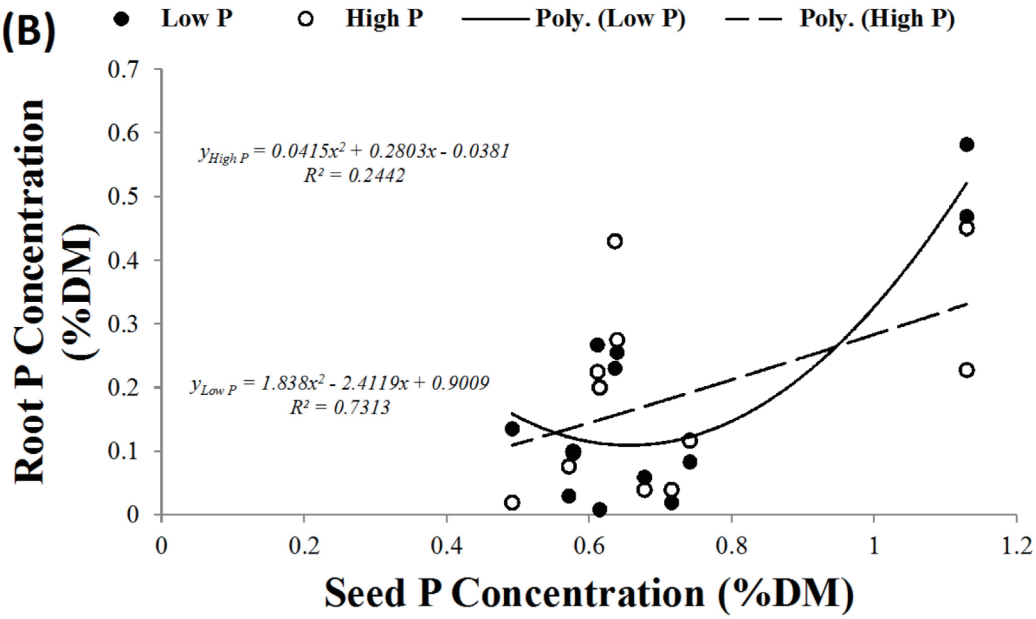
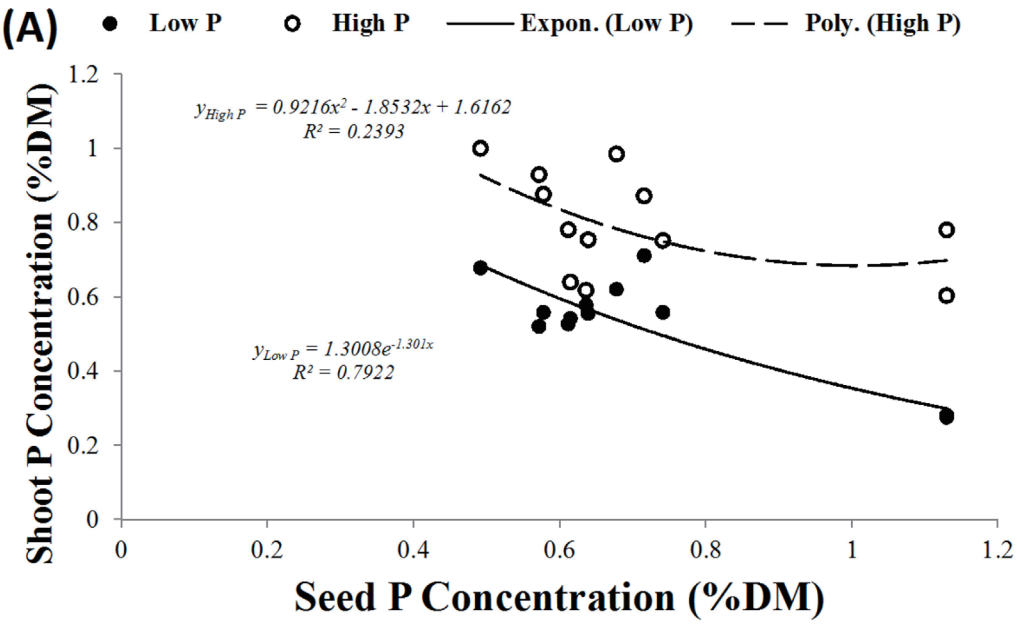




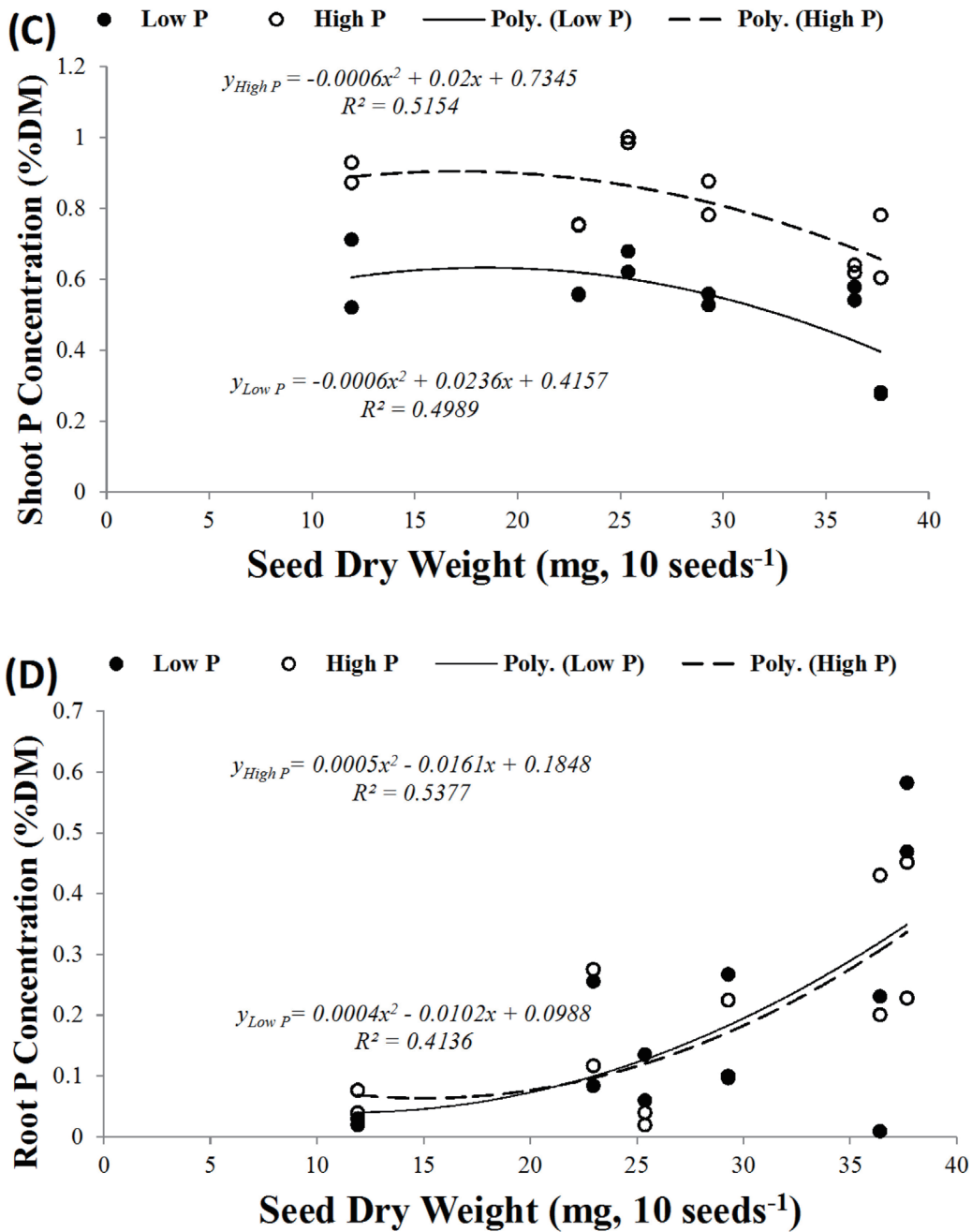
**Supplemental Fig. S1.** Measured (circles) and predicted (lines) values of (A) primary root and (B) total root length of the 12 *Brassica rapa* L. genotypes measured daily for the 15 d following transfer to the phenotyping platform in two independent runs. Predicted values were estimated using a nonlinear mixed-effects model using Supplemental equation S4. (C): Measured (circles) and predicted (lines) values of the elongation rates of lateral roots of the two parents and ten recombinant inbred lines of the *Brassica rapa* L. of the BraIRRI mapping population as a function of the time of their emergence after transfer to the soil-filled rhizoboxes. Predicted values were estimated using a nonlinear mixed-effects model (Supplemental equation S6).



**Supplemental Fig. S2.** (A) Mean diameter of roots of *Brassica rapa* L. genotypes grown for 21 DAT in soil-filled rhizoboxes amended with 0 (white columns) or 600  $\mu\text{M}$   $\text{KH}_2\text{PO}_4$  solution (grey columns); Symbols represent means  $\pm$  s.e.m. ( $n = 12$ ); (B) Volume of root systems of *Brassica rapa* L. genotypes grown for 21 DAT in soil-filled rhizoboxes amended with 0 (white columns) or 600  $\mu\text{M}$   $\text{KH}_2\text{PO}_4$  solution (grey columns); Symbols represent means  $\pm$  s.e.m. ( $n = 12$ ); (C) Root tissue density (Primary axis and columns) and root surface area to root volume ratio (secondary axis and circles) of *Brassica rapa* L. genotypes grown for 21 DAT in soil-filled rhizoboxes amended with 0 (white columns and white circles) or 600  $\mu\text{M}$   $\text{KH}_2\text{PO}_4$  solution (grey columns and black circles). Symbols represent means  $\pm$  s.e.m. ( $n = 12$ ).







**Supplemental Fig. S3.** (A) Relationship between seed P concentration and shoot P concentration, (B) Relationship between seed P concentration and root P concentration, (C) Relationship between seed mass (per 10 seeds each) and shoot P concentration of six *Brassica rapa* L. genotypes grown for 21 DAT in soil-filled rhizoboxes amended with 0 (filled circles) or 600  $\mu\text{M}$   $\text{KH}_2\text{PO}_4$  solution (open circles), (D) Relationship between seed mass (per 10 seeds each) and root P concentration of six *Brassica rapa* L. genotypes grown for 21 DAT in soil-filled rhizoboxes amended with 0 (filled circles) or 600  $\mu\text{M}$   $\text{KH}_2\text{PO}_4$  solution (open circles).

$$N = \frac{4\sigma^2(z_{crit} + z_{pwr})^2}{D^2} \quad (\text{S1})$$

where:  $N$  is the total sample size,  $\sigma$  is the standard deviation of both groups, the  $z_{crit}$  value is the standard normal deviate given in normal score tables and corresponding to the a confidence interval of 95% (1.96), the  $z_{pwr}$  is the standard normal deviate corresponding to 0.80 statistical power and  $D$  is the minimum expected difference between the two means (50%).  $R$  represents the sum of the sample sizes of both comparison groups and  $\sigma$  is assumed to be equal for both groups (Eng 2003).

$$y_{ijk} = m + g_k + ag_{ik} + bg_{jk} + abg_{ijk} + \epsilon_{ijk}, \quad (\text{S2})$$

$$i \in \{1, \dots, n\}, j \in \{1, \dots, r\}, k \in \{1, \dots, s\},$$

$$g_k/ag_{ik}/bg_{jk}/abg_{ijk} \sim N(0, \sigma_{g/ag/bg/abg}^2), \epsilon_{ij} \sim N(0, \sigma^2),$$

where  $y_{ijk}$  represents the root trait from the  $i^{th}$  experimental run,  $j^{th}$  scanner and  $k^{th}$  genotype,  $m$  is the mean trait value,  $g_k$  is the effect of the genotype,  $ag_{ik}$  is the effect of interactions between experimental run and genotypic factors,  $bg_{jk}$  is the effect of interactions between scanner and genotypic factors,  $abg_{ijk}$  is the effect of interactions between experimental run, scanner and genotypic factors,  $\epsilon_{ijk}$  is the residual error,  $n$  is the number of runs (2),  $r$  is the total number of scanners (24) and  $s$  is the number of genotypes (10).

$$\sigma_p^2 = \sigma_g^2 + \frac{\sigma_{ag}^2}{n} + \frac{\sigma^2}{pn} \quad (\text{S3})$$

where  $\sigma_p^2$  = Phenotypic variance;  $p = 6$  is the number of replicates and  $n = 2$  is the number of experiments.

$$y_{ij} = \frac{\phi_{i1}}{1 + \exp[-(DAS_j - \phi_{i2})/\phi_{i3}]} + \epsilon_{ij}, \quad (\text{S4})$$

$$\phi_i = \begin{bmatrix} \phi_{i1} \\ \phi_{i2} \\ \phi_{i3} \end{bmatrix} = \begin{bmatrix} \beta_1 \\ \beta_2 \\ \beta_3 \end{bmatrix} + \begin{bmatrix} b_{i1} \\ b_{i2} \\ 0 \end{bmatrix},$$

$$i = \{1, \dots, s\}, j = \{1, \dots, t\},$$

$$b_{i1} \& b_{i2} \sim N(0, \sigma_b^2), \epsilon_{ij} \sim N(0, \sigma^2).$$

where  $y_{ij}$  is the total root length or primary root length for the  $i^{th}$  genotype, on the  $j^{th}$  DAS, and  $t$  is the number of time-points at which measurements were made (15). The parameters  $\beta_1, \beta_2$  and  $\beta_3$  are the mean values of the individual logistic parameters  $\phi_{i1}, \phi_{i2}$  and  $\phi_{i3}$ , respectively,  $b_{i1}$  and  $b_{i2}$ , are respectively the random effect on the asymptote and inflection point of the logistic function and  $\epsilon_{ij}$  is the residual error. A likelihood ratio test was used to select the final model, which had the three parameters as fixed effects and the asymptote and inflection point as random effects. Autocorrelation in the data was modelled using the moving average (corARMA) and autoregressive model of an order 1 (AR1) correlation structure (Pinheiro and Bates, 2000).

$$Var(\epsilon_{ij}|DAS) = \sigma^2(\delta_1 + |DAS|^{\delta_2}), \quad (\text{S5})$$

where  $\sigma^2$  is the variance when  $j = 0$  and  $\delta_1$  and  $\delta_2$  are the two parameters for the power variance function (Pinheiro and Bates, 2000).

$$y_{ij} = b_{i1} + \beta_1 + \beta_2 DAS_j + \beta_3 DAS_j^2 + \epsilon_{ij}, \quad (\text{S6})$$

$$i = \{1, \dots, s\}, j = \{1, \dots, t\},$$

$$b_{i1} \sim N(0, \sigma_{b_1}^2), \epsilon_{ijk} \sim N(0, \sigma^2).$$

where  $y_{ij}$  is the lateral root growth rate for genotype  $i$  on the  $j^{\text{th}}$  day of the experiment,  $\beta_1, \beta_2$  and  $\beta_3$  are the fixed effect parameters for the quadratic function and  $b_{i1}$  is the random effects on the intercept of the quadratic function.

$$Y_{ijk} = \mu + g_i + \beta_j + \alpha_k + g\alpha_{jk} + \epsilon_{ijk} \quad (\text{S7})$$

$$g_i \sim N(0, \sigma_g^2), \beta_j \sim N(0, \sigma_\beta^2), \alpha_k \sim N(0, \sigma_\alpha^2), \epsilon_{ijk} \sim N(0, \sigma^2)$$

where  $Y_{ijk}$  is the trait value of the  $i^{\text{th}}$  genotype ( $i = 1, 2, \dots, 6$ ) within the  $j^{\text{th}}$  run ( $j = 1, 2$ ) and within the  $k^{\text{th}}$  [P]<sub>ext</sub> treatment ( $k = 1, 2$ );  $\mu$  the overall mean,  $g$  the effect of the genotype,  $\beta$  the effect of the run,  $\alpha$  the effect of [P]<sub>ext</sub> treatment,  $g\alpha$  the genotype by [P]<sub>ext</sub> treatment interaction, and  $\epsilon_{ijk}$  is the residual error.

## References

Eng J 2003 Sample size estimation: how many individuals should be studied? *Radiology* 227: 309-313.  
 Pinheiro JC, Bates DM 2000 *Mixed-effects models in S and S-PLUS*. New York: Springer Verlag.